The Pennsylvania State University

The Graduate School

Department of Bioengineering

FACTORS IMPACTING THE EFFICACY OF CELL-MEDIATED DRUG DELIVERY TO THE BRAIN VIA THE BLOOD BRAIN BARRIER

A Thesis in

Bioengineering

by

Erhan Y. Selvi

Submitted in Partial Fulfillment

of the Requirements

for the Degree of

Master of Science

May 2016

The thesis of Erhan Y. Selvi was reviewed and approved* by the following:

Cheng Dong
Distinguished Professor of Biomedical Engineering
Head of Department of Biomedical Engineering
Thesis Advisor

Justin Brown
Assistant Professor of Biomedical Engineering

William O. Hancock
Professor of Biomedical Engineering
Head of Graduate Program
Honors Advisor

*Signatures are on file in the Graduate School

ABSTRACT

Glioblastoma is the most prevalent primary malignant tumor of the brain and has a very poor prognosis of death usually occurring within 2 years at the most (Stupp et al., 2005). Cell-mediated drug delivery to the brain is a new field of treatment and the blood-brain barrier plays a vital role in delivery of drugs to the brain. The binding of vascular cadherin's (VE-cadherin) cytosolic domain with intracellular catenins was shown to be an important aspect in the cell's ability to limit permeability and maintaining its junctional strength (Navarro et al., 1995). Previous studies have shown VCAM-1/VLA-4 binding to induce VE-cadherin breakdown (Khanna et al., 2010). Gap formation in the endothelium with respect to time and the presence of immune cells or cytokines was examined in this study, as well as the compatibility of the immune cells for a model of cell-mediated drug delivery with a chemotaxis study. Gap formation due to co-culture with Jurkat cells was significant but not with THP-1 cells. Additionally, gap formation was not time dependent. VE-cadherin breakdown due to endothelium stimulation from tumor necrosis factor alpha (TNFα) for 24 hours resulted in increased gap formation when cultured with Jurkat cells, but not THP-1 cells. Cell adhesion molecules were most not expressed on the endothelium after 24 hours of TNFα exposure then 24 hours with no exposure. White blood cells (WBCs) isolated from human blood did not result in significant gap formation with the endothelium as well. Chemotaxis studies showed Jurkat cells to be the better candidate for cell-mediated drug delivery since it migrated more effectively through 8μm pores. Overall, Jurkat cells prove to be a better candidate for drug delivery in terms of gap formation and migration.

TABLE OF CONTENTS

LIST OF FIGURES

LIST OF TABLES

ACKNOWLEDGEMENTS

I would like to thank Dr. Cheng Dong for allowing me to conduct research in his lab, for his help in the completion in my thesis, and for his guidance and counseling.

I would also like to thank the committee members, Dr. Justin Brown and Dr. William Hancock, for agreeing to be a part of my committee and their guidance in the completion of my thesis.

Thank you to Virginia Aragon-Sanabria and Gloria Kim for their help with conducting and planning out the experiments, and learning the techniques necessary for success in the lab.

Finally, thank you to my family and friends for their cooperation, comfort, and comradery.

Chapter 1

Background

1.1 Cancer Statistics

Cancer is one of the most devastating diseases in the history of mankind and is the second leading cause of death in the United States. It was projected that over 1.6 million new cases and over 500,000 cancer deaths would occur in the United States in 2015 alone (Siegel et al., 2015). Forty-three % of men and 38 % of women will develop an invasive form of cancer in his or her lifetime. The likeliness to get cancer is both based on random genetic mutations and lifestyle choices. However, many lifestyle choices such as smoking or exposure to radiation may alter these prevalence statistics (Siegel et al., 2015).

1.2 Brain Cancer

Cancer is widely accepted as the presence of a collection of six main characteristics: self-sufficiency in growth-signals, insensitivity to growth-inhibitory signals, evasion of programmed cell death, limitless replicative potential, sustained angiogenesis, and tissue invasion and metastasis (Cavallo et al., 2011). Out of these traits, metastasis plays a major role in the severity of cancer diagnoses – 90% of cancer deaths may be attributed to metastases (Sporn, 1996). The metastasis process involves the cancer cell migrating away from the location of the primary (initial) tumor, entering the blood

circulation, extravasating out of the blood stream into a distant location in the body, and colonization of the previously healthy tissue (Chambers et al., 2002; Wyckoff et al., 2000).

Brain cancers can be the result of a primary brain tumor or metastatic lesions as a result of other cancers. Glioblastoma is the most prevalent primary malignant tumor of the brain and has a very poor prognosis of death usually occurring within 2 years at the most (Stupp et al., 2005). On the other hand, non-small cell lung cancer, breast cancer, small cell lung cancer, and melanoma are all known to metastasize to the brain and form secondary tumors (Nussbaum et al., 1996).

1.3 Cancer Treatments

There are several options for the treatment of glioblastoma. Methods such as surgery, Carmustine Wafers, and radiation have been used to treat glioblastoma for years now and are well established (Ekeblad et al., 2007; Preusser et al., 2011; Stupp et al., 2005). Newer methods are being researched that include targeted therapy and immunotherapy that look to increase the efficiency of drug delivery (Chertok et al., 2008). Determining which treatment should be used depends on the stage of the cancer and what kind of success other treatment methods are having. However, each method of treatment has its complications and this is why new methods must be explored.

For newly diagnosed patients, the first step in treatment is usually surgical removal of the tumor. Conventional MRI, functional MRI, and diffusion tensor imaging sequences are all tools that help surgeons plan out and complete the surgery. This method

is not completely effective though, because often times lingering tumor cells exist in other parts of the brain tissue that cannot be clearly removed like the primary tumor mass (Preusser et al., 2011).

Another option for treatment are Carmustine Wafers. Carmustine (1,2-bis[2-chloroethyl]-1-nitrosourea) Wafers are biodegradable wafers that are placed within the tumor bed during surgery. The drug is then released over a 3-week period and it is generally considered a safe treatment. However, there have been several reported issues with this treatment method, including cerebrospinal fluid leakage, intracranial infections, and seizures (Preusser et al., 2011).

Currently, the most popular method of treatment for glioblastoma is a combination of radiotherapy and then treatment with Temozolomide. Radiotherapy treatment generally consists of 2 Gy per fraction given once a day, 5 days a week, for 6 weeks. The radiotherapy is guided by computed tomography scans and delivered to the main tumor volume with a 2 to 3 cm margin. Temozolomide is a proven antitumor drug that targets DNA repair enzymes in cancer cells. While radiotherapy is relatively targeted, Temozolomide treatment is a standard chemotherapeutic medicine so it comes with many of the associated side effects: nausea, fatigue, and hematological toxicities (Ekeblad et al., 2007; Stupp et al., 2005).

1.4 Blood-Brain Barrier

The blood-brain barrier plays a vital role in maintaining the health of the human brain. Anything that flows in the blood stream (blood cells, nutrients, waste products) has

the possibility of entering the tissue at the site of the capillaries where the vascular endothelium is only one-cell thick. For muscles and most other tissues where there is high metabolic activity, this one-cell thick capillary barrier is evolutionarily important because it allows for quick diffusion of the nutrients or wastes between the blood vessels and the tissues. However, the brain is a very sensitive organ and because of this, the capillaries that run through the cerebral tissues a much more fortified compared to most other capillaries in different parts of the body.

The fundamental structure of the blood-brain barrier is called the neurovascular unit. Starting from the lumen of the capillary and proceeding outwards, the cells and structures present in the neurovascular unit are the capillary, basal lamina, pericyte, astrocytic perivascular endfeet, and finally neuronal axons (Figure 1.1).

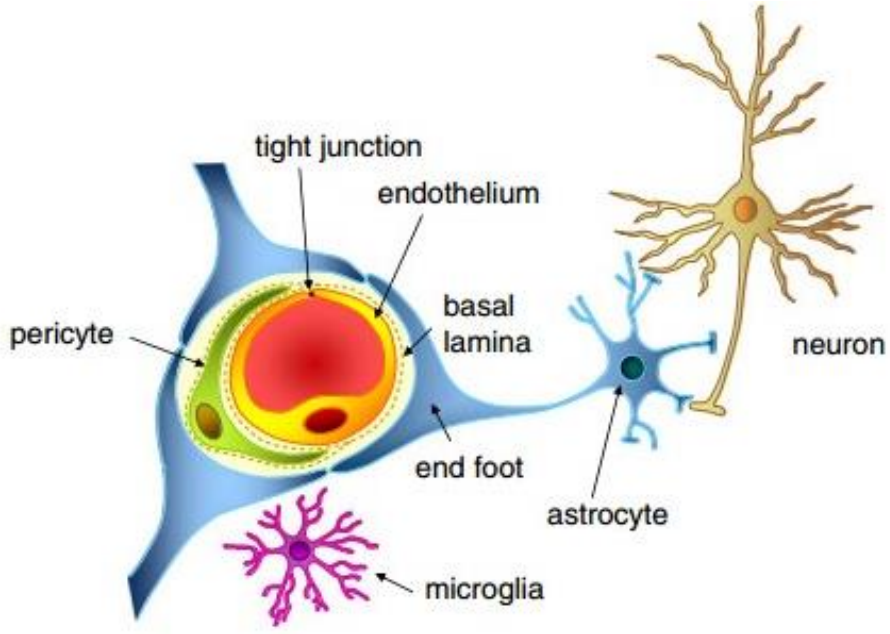

Figure 1.1 The neurovascular unit at the capillary level. Starting at the innermost part is the lumen which is surrounded by the one-cell thick endothelial capillary. Next is the basal lamina and the pericyte. Surrounding these structures are the astrocytic endfeet. Connected to the astrocytes are the neuronal axons (Abbott, 2013).

The blood-brain barrier integrity is important to keeping harmful waste products outside of the brain, as well as to maintain normal ionic balances in the neuronal environment so as to not imbalance the systems meant to send action potentials from neuron to neuron (Cserr and Bundgaard, 1984). What governs this strict barrier between the blood flow and the brain tissue that is unique to the blood-brain barrier is the complexity of the tight junctions of the endothelial capillaries. Transendothelial resistance (TEER) of normal capillaries is usually about 2-20 ohm.cm^2, compared to at least 1,000 ohm.cm^2 observed in the blood-brain barrier capillary endothelium (Butt et al., 1990). While the tight junctions play the unique role in the blood-brain barrier endothelium, adherens junctions are also present between the endothelial cells and help create a tight binding of the cells together (Figure 1.2) (Abbott et al., 2006).

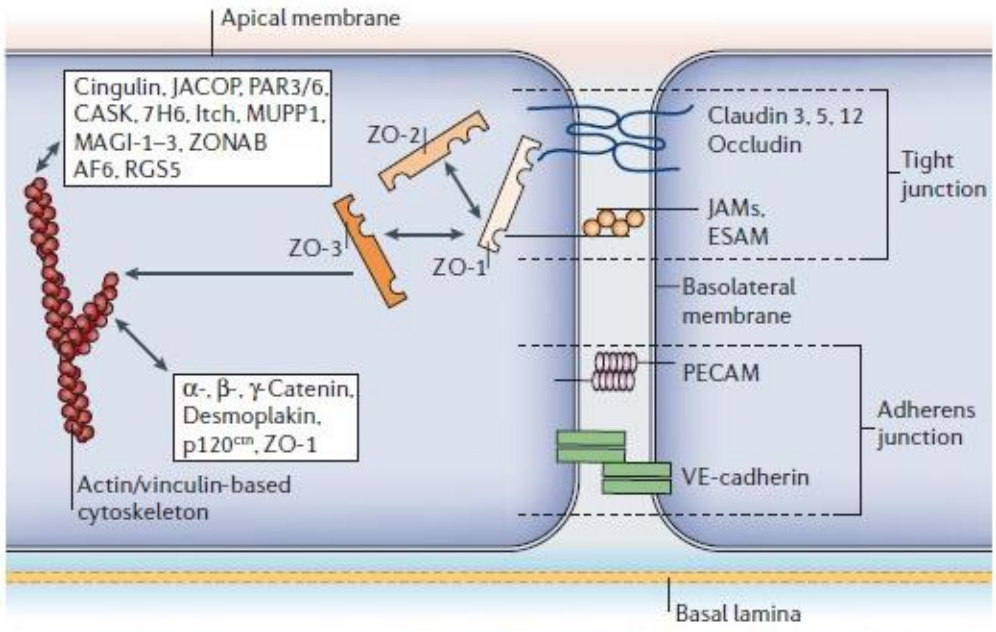

Figure 1.2 The molecular structure of the blood-brain barrier endothelium. Cellular adhesion molecules that make up the intercellular bond include the tight junction molecules (claudin 3,5,12, occludin, junctional adhesion molecules (JAMs), endothelial selective adhesion molecule (ESAM)), and adherens junctions (platelet-endothelial cell adhesion molecule (PECAM), and vascular endothelial cadherin (VE-cadherin)) (Abbott et al., 2006).

1.4.1 VE-Cadherin

Out of the many types of cellular adhesion molecules present at the interface between the endothelial capillaries, vascular endothelial cadherin (VE-cadherin) is considered one of the more important molecules that makes up the intercellular binding domain. Cadherins are a type of cellular adhesion molecule that are involved in homotypic cell-cell binding in a calcium dependent manner (Navarro et al., 1995). They are transmembrane proteins that have a cytoplasmic and cytosolic domain. VE-cadherin has a cytosolic domain that binds to several other proteins including β-catenin, p120, and plakoglobin; these interactions are important for the signaling that occurs between the cytosolic domain of VE-cadherin and the cytoskeleton of the cell (Bravi et al., 2014). β-catenin binds to α-catenin, which in turn binds to the actin cytoskeleton and interacts with α-actinin, ajuba, zonula occludens-1 (ZO-1), and other proteins that all play a role in the stability of the cytoskeleton and the cellular adhesion molecules (Weis and Nelson, 2006). Furthermore, the binding of VE-cadherin's cytosolic domain with intracellular catenins was shown to be an important aspect in the cell's ability to limit permeability and maintaining its junctional strength (Navarro et al., 1995). The significance of VE-cadherin in this project is that it is found in the microvasculature of the blood-brain barrier as well (Vestweber, 2008).

1.5 Endothelial Cytoskeleton

The cytoskeleton gives a cell its shape and plays an important role in the structural integrity of the cell itself as well as maintaining a proper barrier with its

neighboring cells in the case of the endothelium. There are three main proteins that make up the cytoskeleton: actin filaments, intermediate filaments, and microtubules (Ingber, 1993). The actin filaments have been shown to be perhaps the most important structure of the cytoskeleton when it comes to permeability of the vasculature when studies have shown that cytochalasin D, an actin filament disrupter, increases the permeability of the endothelium (Shasby et al., 1982). Agonist induced barrier dysfunction is believed to be the result of phosphorylation of myosin light chain proteins which are catalyzed by calcium/calmodulin dependent myosin light chain kinase. This causes the endothelial cells to contract through the formation of actin stress fibers, resulting in gaps between adjacent cells (Dudek et al., 2001).

1.6 Transendothelial Migration of Leukocytes

Leukocytes are known to be able to migrate from the blood flow in the capillaries to the tissue through the endothelial cells of the vasculature. This process is required for leukocytes to be able to migrate towards sites of inflammation and disease to combat potential pathogens. The process begins with the leukocyte being captured on the endothelial cell via selectins. Next, it will continue to roll on the endothelium in the direction of the blood flow. During this rolling phase, the leukocyte gets further activated and the rolling begins to slow down until the cell eventually is arrested on the endothelium. At this point, the bonds between the leukocyte and the endothelial cell strengthen and the leukocyte begins to crawl through the endothelium. At this point, the leukocyte could begin to migrate either through a single endothelial cell, which is known

as transcellular migration, or between two contiguous endothelial cells, which is known as paracellular migration below (Figure 1.3) (Ley et al., 2007).

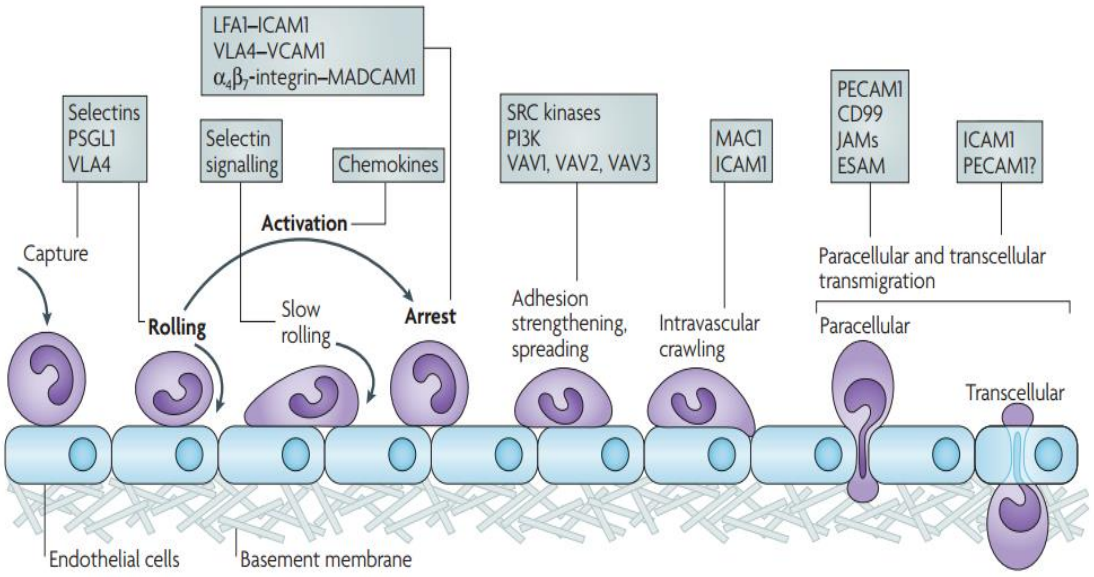

Figure 1.3 The process of endothelial transmigration and the cellular adhesion molecules involved. The steps include capture activation, adhesion, crawling, and finally either paracellular or transendothelial migration (Ley et al., 2007).

It has been shown that the cellular adhesion molecule, platelet endothelial cellular adhesion molecule (PECAM-1), is required for leukocyte migration into the tissue (Muller et al., 1993).

1.6.1 Cellular Adhesion Molecules

Cellular adhesion molecules play an important role in leukocyte binding to endothelial cells and subsequent transendothelial migration. Intercellular adhesion molecule 1 (ICAM-1) is a cellular adhesion molecule, a member of the immunoglobulin superfamily, that is widely expressed by endothelial cells (Staunton et al., 1988).

Endothelial cells are stimulated to increase ICAM-1 expression when they are exposed to lipopolysaccharides and cytokines; this induced expression occurs on the time scale of hours (Lawrence and Springer, 1991).

Vascular cell adhesion molecule 1 (VCAM-1) is a cellular adhesion molecule that is often expressed on endothelial cells of the vasculature. Thus, these proteins are known to make up the lining of the blood vessels (Elices et al., 1990). It is classified as a part of the immunoglobulin gene superfamily just as ICAM-1 (Osborn et al., 1989). Expression of VCAM-1 on the surface of vascular endothelial cells is increased in the presence of cytokines which are released from the tissue in inflammatory conditions as well (Elices et al., 1990).

1.6.2 Integrins

Lymphocyte function-associated antigen 1 (LFA-1) is an integrin that is widely expressed on leukocytes. It is made up of the proteins CD11a and CD18 which make up its α and β subunits respectively. It has been proven that ICAM-1 is the ligand for LFA-1 through *in vitro* testing with artificial membranes coated with ICAM-1 that resulted in extremely specific binding of lymphocytes that express LFA-1 to the membrane (Marlin and Springer, 1987). Macrophage-1 antigen (Mac-1) is another integrin expressed on leukocytes that can bind to ICAM-1. Its α and β subunits are CD11b and CD18 respectively. This interaction proves that cellular adhesion molecules of the immunoglobulin superfamily can have multiple ligands since ICAM-1 can bind to both LFA-1 and Mac-1. However, it was shown that the interaction between LFA-1/ICAM-1

interaction and the Mac-1/ICAM-1 interaction were different in their interaction sites on ICAM-1 (Diamond et al., 1990). It has been suggested that these interactions play an important role in the transendothelial migration of leukocytes, and previous experiments have been conducted that showed decreased speed, track length, and displacement of neutrophils expressing LFA-1 and Mac-1 on pericytes expressing ICAM-1 (Proebstl et al., 2012).

Another type of integrin is very late antigen - 4 (VLA-4). VLA-4 is part of the β_1 integrin family that is associated with cell attachment to the extracellular matrix. Similar to how LFA-1 and Mac-1 complement the ICAM-1 receptor as mentioned above, VLA-4 is the ligand for VCAM-1. The interaction between VLA-4 and VCAM-1 is best seen with lymphocytes and endothelial cells and proves that β_1 integrins can participate in cell-cell binding as well. It has also been proven that the VLA-4/VCAM-1 binding occurs separately from the VLA-4/fibronectin (Fn) interaction (Elices et al., 1990). It has been previously shown in our lab that VE-cadherin disassembly is mediated by the VLA-4/VCAM-1 interaction in the case of tumor cell extravasation (Peng et al., 2005).

1.7 Cell-Mediated Drug Delivery

Cell-mediated drug delivery is a growing field of immunotherapy. The basic concept is to harvest immune cells and load them with the drug of interest to act as a carrier to bring the drug to the site of the disease or ailment in an active targeting manner. There are numerous reasons as to why this method is becoming a popular method of drug delivery. The first is that sites of pathology are often accompanied by inflammation, and

multiple types of leukocytes have the chemotactic ability to be recruited to the site of pathology. This makes cell-mediated drug delivery a more targeted therapy that is also more efficient in terms of drug concentrations used since less will theoretically lost into the blood stream. Another advantage is that certain leukocytes such as monocytes, macrophages, and neutrophils are phagocytic and will readily uptake drugs that are encapsulated in nanoparticles or in solution with the blood as a colloidal suspension. A third important factor is that a large amount of the drug can be placed into the nanoparticle or carrier of interest, which is then conjugated with the cell. Other aspects include the potential for use of a magnetic field to attract immune cells with magnetic particles and localize them to a certain part of the body, and the possibility that cell-mediated drug delivery will block the entrance of other pathogens to the region of pathology (Chen and Liu, 2012).

Overall, this process will prove to be a difficult task to overcome, especially with the tight vasculature of the blood-brain barrier. However, if we seek to understand the gap formation process and chemotactic ability of immune cells even further, it can become a real solution to glioblastoma, and other cancers affecting the millions of humans around the world.

1.8 Goals of this Study

The goals for this study will be to create a model for drug delivery via the blood-brain barrier and determine which type of immune cell would serve as the better candidate to deliver drugs through the blood-brain barrier and ultimately to the brain

tissue. The immune cells of interest are monocytes and lymphocytes, as well as an entire population of white blood cells (WBCs). For each of these immune cell groupings, they're ability to migrate through the blood-brain barrier will be evaluated by their ability to induce VE-cadherin disassembly. VE-cadherin disassembly will be evaluated by a combination of percent gap formation and number of gaps formed. Along with gap formation, the chemotactic ability of the monocytes and lymphocytes will be examined to determine which cell line will migrate to the site of drug delivery more effectively. To complete this study for generating a model for drug delivery to the brain, experiments should be conducted that look at how well the drug can be conjugated or encapsulated in the immune cell of interest.

Chapter 2

Materials and Methods

2.1 Cell Culture

Bovine Brain Microvascular Endothelial Cells (BBMVECs) were cultured in Bovine Brain Endothelial Cell Media, both obtained from Cell Applications, Inc (San Diego, CA). THP-1 line TIB-202 cells (THP-1), a human monocyte cell line, were obtained from American Type Culture Collection (ATCC) and were cultured in RPMI 1640 medium (Invitrogen) supplemented with 10% fetal bovine serum (FBS) (Atlanta Biologicals) and 100 units /mL penicillin-streptomycin (pen-strep) (Invitrogen). Jurkat T-cell clone E6 cells (Jurkat), a human T lymphocyte cell line, were obtained from ATCC and maintained in RPMI 1640 + 10% FBS and 100 units/mL pen-strep. Cells were maintained at 37°C and 5% CO_2 in a humidified incubator.

Fresh human blood was collected from healthy adults under informed consent. Venipuncture was performed by the nursing staff at the Penn State Clinical Research Center and blood was collected into EDTA-coated Vacutainer® (Becton Dickinson). WBCs were isolated using a double gradient with Histopaque® 1119 and 1077 (Sigma) as described by the manufacturer. The isolated WBCs were cultured in RPMI 1640 + 10% FBS and 100 units/mL pen-strep and used immediately for experiments.

2.2 Endothelial - Leukocyte Co-culture

Glass coverslips were first sterilized with 70% ethanol for 15 minutes and washed twice with phosphate buffered solution (PBS) for 10 minutes and placed into 6-well culture dishes. At this point, the glass coverslips were coated with fibronectin at a concentration of 10µg/mL and were stored at 4°C overnight for the use the next day. BBMVECs were then lifted from their petri dishes using 0.25% trypsin (Invitrogen) and 3mL of the solution containing cells and BBMVEC culture media were seeded onto the glass coverslips at a concentration of 6.0×10^4 cells/mL for each well. At this point, the BBMVEC cells were allowed to culture in an incubator for 3 days until they reached confluency on the glass coverslips. During the second day of this period, the BBMVEC culture media was replaced with hydrocortisone supplemented media at a concentration of 2.67µL/mL and allowed to culture for the remaining 24 hours of the 3-day period. For experiments involving tumor necrosis factor – α (TNFα), TNFα was added to the endothelial layer after the third day of culturing in the incubator (when the BBMVEC monolayer has already reached confluency) and was allowed to culture for its specified amount of time and concentration based on the experiment. THP-1, Jurkat, and WBCs were seeded onto the BBMVEC monolayers at a seeding density ratio of 1:1 for all co-culture experiments. The THP-1, Jurkat, and WBCs were seeded into the well plates in the BBMVEC growth media.

2.3 VE-Cadherin Cell Staining

After the specified amount of time for co-culture, the media in the well plates containing the leukocytes was aspirated and the monolayer was immediately fixed with 4% formaldehyde (Sigma), then washed twice with PBS for 5 minutes each. The cells were then made permeable with 0.3% Triton-X in PBS (with 5% goat serum) for 1 hour at room temperature on a rocker. At this point, anti-VE-Cadherin (Cell Signaling) was added at a concentration of 10µg/mL to the glass slides and were allowed to culture overnight at 4°C. The next day, the slides were stained at 1 µg/mL concentration of Alexa Fluor 488 for 1 hour at room temperature in the dark, 2µg/mL concentration of Hoechst solution for 15 minutes at room temperature in the dark, and finally the coverslips were washed three times with PBS and mounted onto glass slides and stored at 4°C until they were ready for imaging.

2.4 VE-Cadherin Disassembly Analysis

Cell imaging was performed using a Nikon fluorescence microscope. Each coverslip was viewed under a 100x objective and 24 images were taken per slide in an organized yet non-selective (random) field of view. The corresponding images were then analyzed with ImageJ software. The area of the gaps between the endothelial cells was calculated by imageJ (Rasband, 1997). For each of the 24 images, a gap percentage was calculated that was equal to the sum of pixels that were gaps in image of the endothelium divided by the total number of pixels in the image, which was 1,447,680 pixels. The average endothelial gap was then calculated from the 24 images per slide and plotted.

Gap formation is directly related to VE-cadherin disassembly because gaps did not show any fluorescence locally when the VE-cadherin was not intact. Thus, when endothelial cells formed a tight monolayer with no gaps, the border between two cells would fluoresce, yet when gaps formed, VE-cadherin would not be present at the membranes and therefore unavailable for the antibodies to bind to, resulting in a lack of fluorescence.

2.5 Gap Size Analysis

Gap size was determined using the Nikon imaging software that showed the relationship between 1 pixel in the image and the actual length represented in the image. The scale provided by the program indicated a 0.06μm/pixel ratio. Therefore, approximate areas of the gaps were able to be calculated using the measurements from the VE-cadherin disassembly analysis of gaps. Gaps with an approximate diameter of 3μm or greater were the only gaps of interest. Using the raw data of pixel area that was quantified, gaps greater than the 3μm diameter threshold were selected for analysis of gap number and this value was compared between the different cell lines used and as well as a function of time within a cell line.

2.6 Boyden Chamber Chemotaxis Assay

For the chemotaxis study conducted on THP-1 and Jurkat cells, a 48-well Boyden chamber was used. The bottom wells were filled with Monocyte Chemoattractant Protein-1 (MCP1) to act as a chemoattractant. A polyvinylpyrrolidone-free carbonate

filter with 8µm pores (Neuroprobe) was placed on top of the bottom wells. Next, a silicone gasket was placed on top of the filter and the bottom wells and then the top portion of the chamber was screwed on tightly on top of the gasket to complete the assembly. The top portion of the Boyden chamber contains wells that connect to the bottom wells through the gasket to allow for cells to migrate through the filter. THP-1 and Jurkat cells were seeded into the top wells of the chamber at concentration of 16,000 cells/mL as per the protocol provided by the manufacturer of the chamber, based on the filter being used. The set-up of the chamber can be seen in Figure 2.1 below.

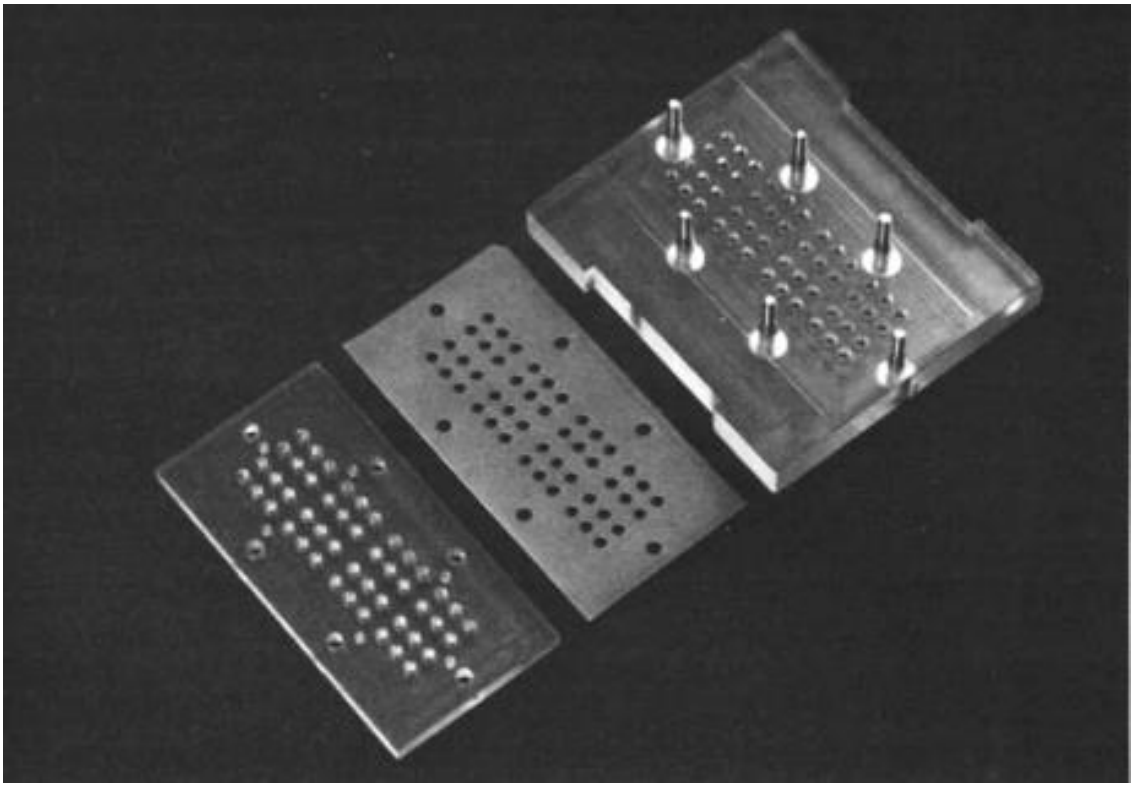

Figure 2.1 48-well Boyden Chamber components. From left to right: top well chamber, silicone gasket, and bottom well chamber (Falk et al., 1980).

The chamber was then placed in the incubator at 37°C and 5% CO_2 for the specified amount of time for the cells to migrate. Upon completion of the experiment, the top side of the filter was first scraped to remove any cells that did not migrate through the pores, then it was fixed and stained using a Hemacolor® Stain Set following the prescribed protocol, and the stained filter was then placed on a glass slide at which point it was ready for imaging. Slides were imaged under 20x brightfield and the number of cells migrated in the frame were counted and represented as number of cells migrated per mm^2.

2.7 Statistical Analysis

All results were represented as means ± SEM. One-way ANOVA was used for comparisons between multiple groups and two-sample T-test for comparisons between two groups. Results were considered statistically significant at $p \leq 0.05$.

Chapter 3

Results

The purpose for these studies is to determine which immune cell type will act as a more suitable carrier for drugs through the blood-brain barrier, thus creating a model for cell-mediated drug delivery to the brain. Co-culture studies were conducted between BBMVEC and Jurkat or THP-1 to determine the presence of signaling between the cells or not. Gap formation via VE-cadherin disassembly is also used as an indicator for the immune cell's ability to migrate via the paracellular route. Further co-culture studies were run to examine how the BBMVEC monolayer responds in an inflammatory state, which was accomplished with the addition of recombinant TNFα to the co-culture. Migration studies were also conducted to determine if the cells of interest will migrate to the site of inflammation which will provide a clearer picture to the entire cell-mediated drug delivery process of gap formation and subsequent migration.

3.1 Endothelial – Leukocyte Co-Culture Study

To determine the role that certain white blood cells play in VE-cadherin disassembly and to see if there is any type of signaling communication between the cells, a gap formation study was conducted. A BBMVEC monolayer was grown to confluency before the addition of Jurkat cells or THP-1 cells, at which point the cells were co-cultured for the specified amount of time (2 hours, 4 hours, and 8 hours). Images of the

monolayer exposure to Jurkat cells at the various time points can be seen in Figure 3.1, and the monolayer's response to THP-1 is shown in Figure 3.2

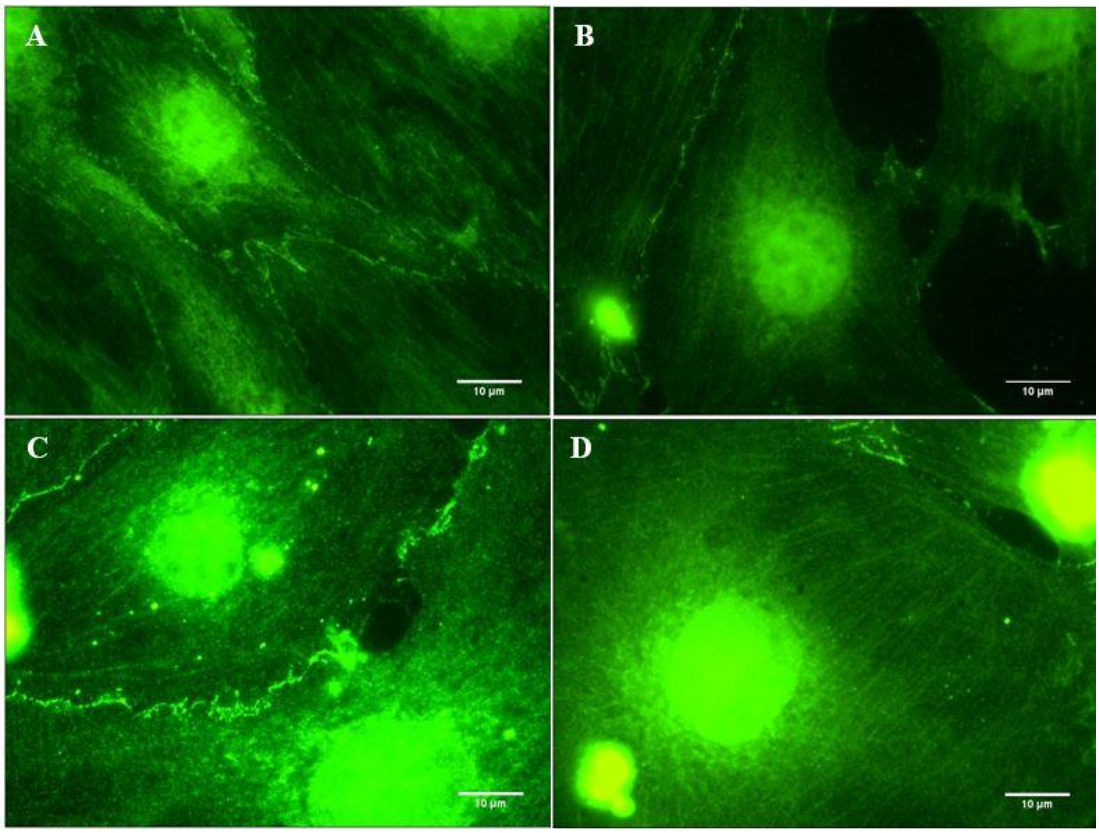

Figure 3.1 Images of gap formation in BBMVEC Jurkat co-culture. A – No exposure to Jurkat; B – 2 hours of co-culture; C – 4 Hours of co-culture; D – 8 Hours of co-culture. Representative images were examined and show intact VE-cadherin junctions at sites of green fluorescent borders and VE-cadherin disassembly where there are no green fluorescent borders.

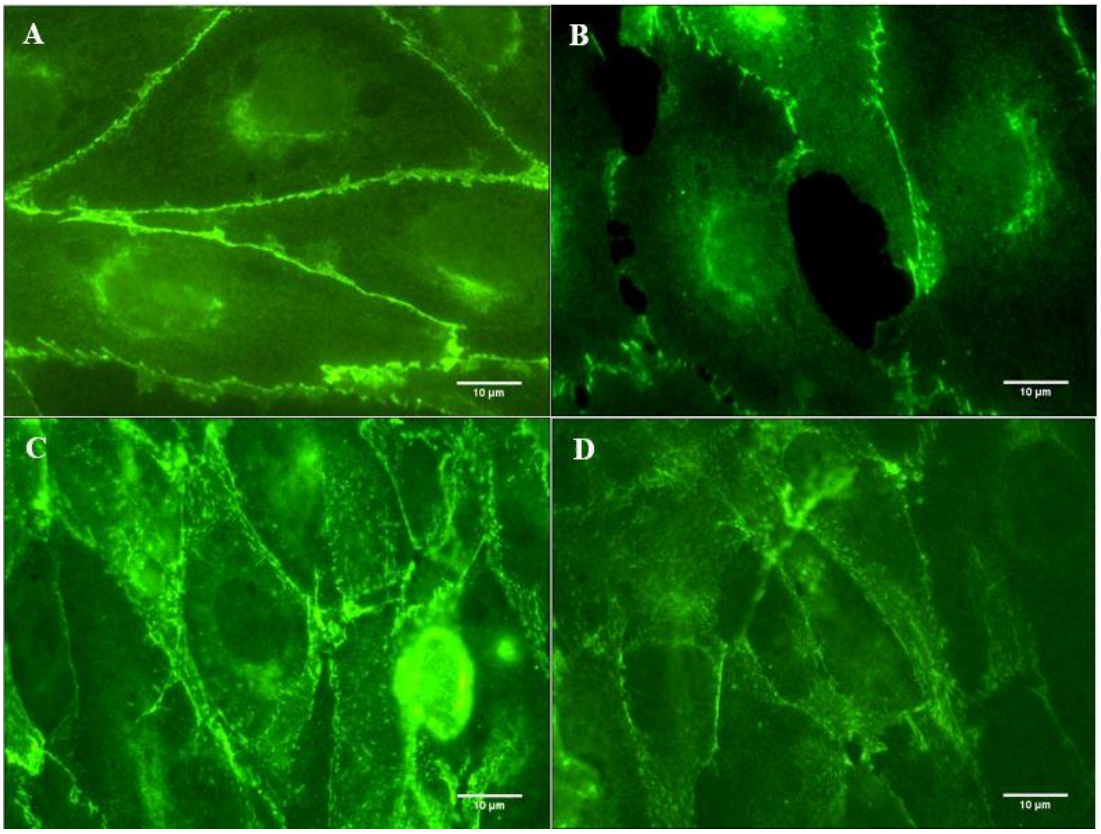

Figure 3.2 Images of gap formation in BBMVEC THP-1 co-culture. A – No exposure to THP-1; B – 2 hours of co-culture; C – 4 Hours of co-culture; D – 8 Hours of co-culture. Representative images were examined and show intact VE-cadherin junctions at sites of green fluorescent borders and VE-cadherin disassembly where there are no green fluorescent borders.

When the gap formation for exposure to Jurkat or THP-1 cells for all time points is grouped together against no exposure to either cell line, there is a significant increase in gap formation when the monolayer is exposed to Jurkat cells versus THP-1 cells. The total gap formation percentage for Jurkat cells over all time points is 3.36% while the gap formation due to THP-1 cells is 1.60%. The results for these points is represented in Figure 3.3 below.

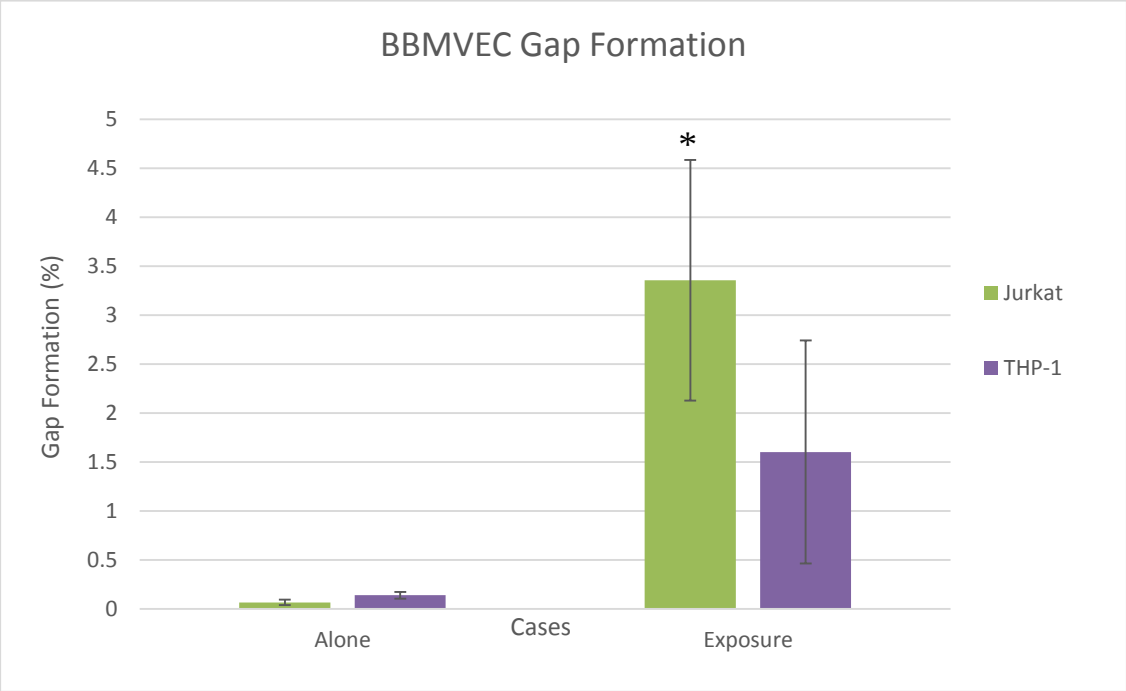

Figure 3.3 Endothelial gap formation in BBMVEC in response to co-culture with Jurkat or THP-1 cells. Alone represents a case with no exposure to Jurkat or THP-1 cells; Exposure represents a case where gap formation in the presence of the respective cells for multiple time points. * indicated $p < 0.05$ for Jurkat Exposure with respect to Jurkat Alone. Values are means ± SEM for n = 3.

Expanding this study out to look at the gap formation at each of the time points, the BBMVEC Jurkat co-culture time course results are represented in Figure 3.4 below. The same type of results for the BBMVEC THP-1 co-culture is seen in Figure 3.5.

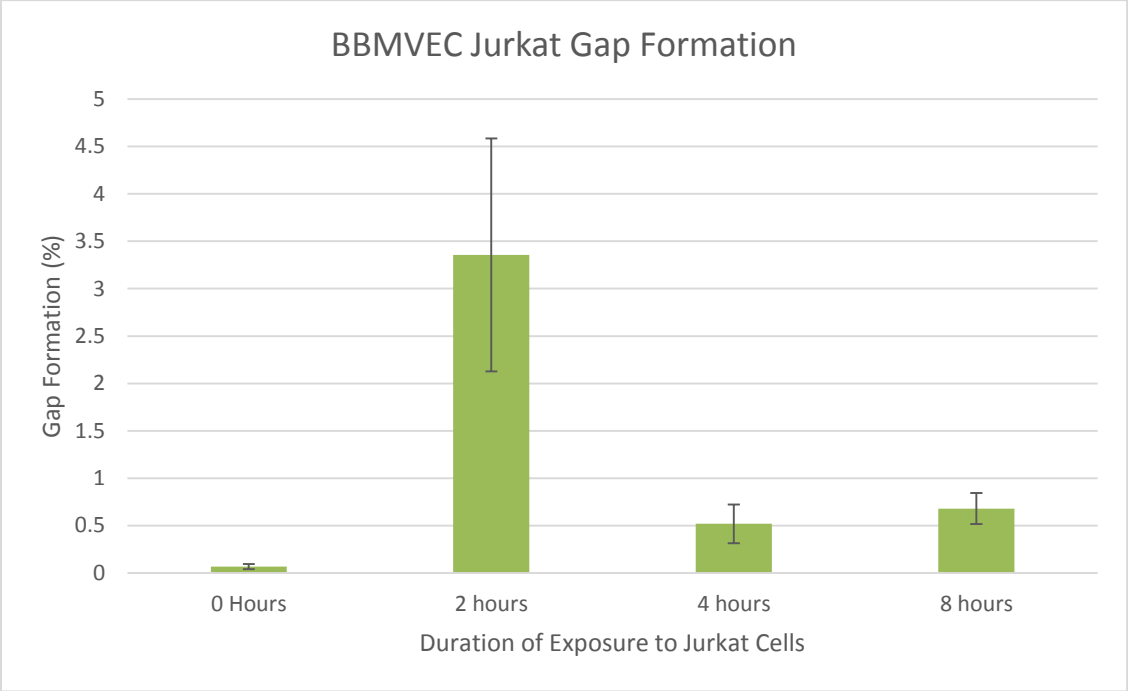

Figure 3.4 Endothelial gap formation in BBMVEC in response to co-culture with Jurkat cells for 2 hours, 4 hours, and 8 hours. Negative represents a case with no exposure to Jurkat cells. One-way ANOVA showed that the gap formation between the cases were not significant for all time points and the p-value > 0.05. Values are means ± SEM for n = 3.

It was found that compared to no exposure to Jurkat cells, the gap formation is not statistically significant as a function of time. While the gap formation percentage was significant when the values for 2 hours, 4 hours, and 8 hours were lumped together when compared to the control of no exposure to the Jurkat cells, when they are separated and looked at individually, the values did not differ significantly. Gap formation is the largest at 2 hours with a value of 3.36% and then decreases with added time. The 4-hour time point had 0.52 % gap formation and the 8-hour time point had 0.68 % gap formation.

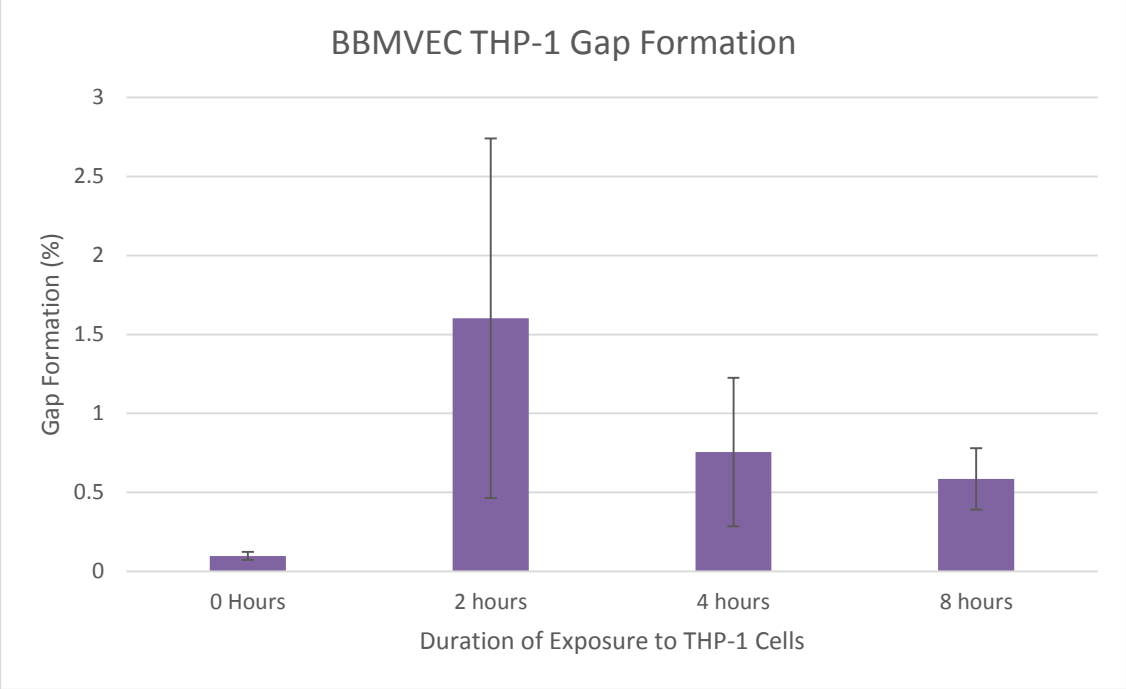

Figure 3.5 Endothelial gap formation in BBMVEC in response to co-culture with THP-1 cells for 2 hours, 4 hours, 8 hours. Negative represents a case with no exposure to THP-1 cells. One-way ANOVA showed that the gap formation between the cases were not significant for all time points and the p-value > 0.05. Values are means ± SEM for n = 3.

For the BBMVEC and THP-1 co-culture, the gap formation as a function of time is also not statistically significant. Although the differences were not significant, there is a clear trend of decreasing gap formation with time, just as the case with the Jurkat cells on the BBMVEC monolayer. Maximum gap formation was 1.60 % which was seen at the 2-hour time point, followed by 0.76 % at the 4-hour time point. The 8-hour time point had the smallest value of 0.58 %.

Comparing the gap formation at each time point between each cell line can potentially show which cell line has the larger effect on BBMVEC gap formation. Figure 3.6 below shows the data portrayed in Figures 3.4 and 3.5 together. Jurkat gap formation was larger than THP-1 gap formation at all time points except for 4 hours where the

difference is very minimal. However, it must be acknowledged that these differences were not significant.

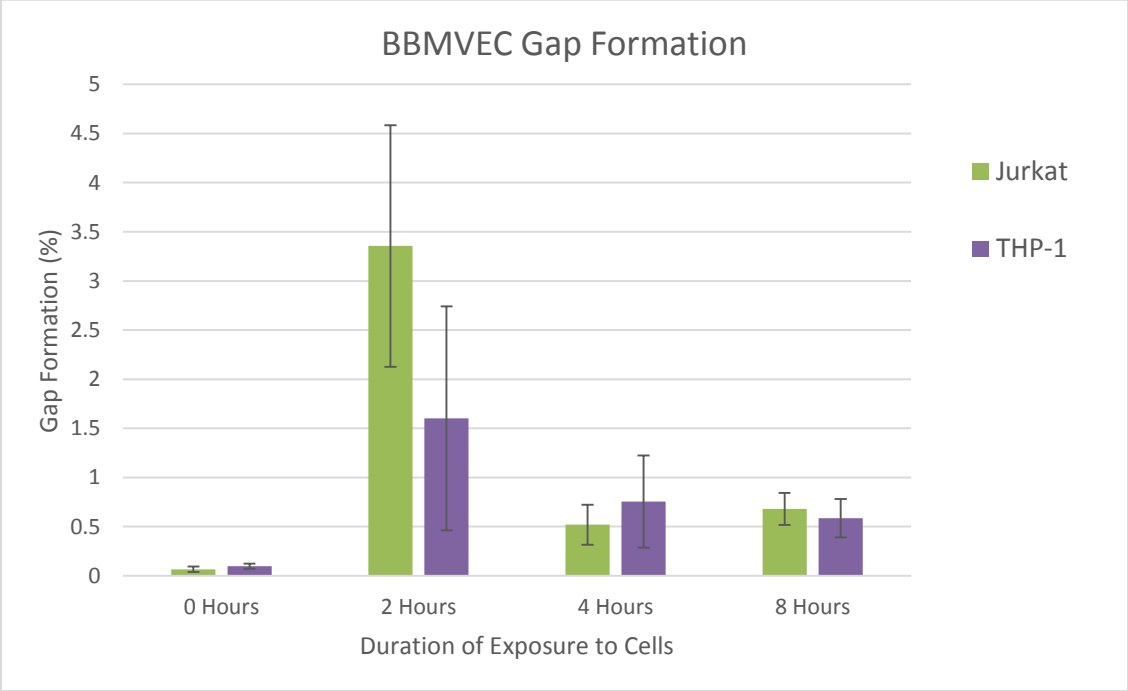

Figure 3.6 Endothelial gap formation in BBMVEC in response to co-culture with Jurkat and THP-1 cells for 2 hours, 4 hours, 8 hours. Negative represents a case with no exposure to either cell line. One-way ANOVA showed that the gap formation between the cases were not significant for all time points and the p-value > 0.05. Values are means ± SEM for n = 3.

In an effort to further understand the type of gap formation in the BBMVEC monolayer, the number of gaps formed, categorized by how large they were, was analyzed as well. Also, to more accurately correlate the gap formation and VE-cadherin disassembly with transendothelial migration, gaps that were only larger than 3µm in diameter were counted for this study. Gap size was determined using the conversion ratio of 0.06µm/pixel as provided by the imaging software for the 100x objective, and solving for the number of pixels in an area of a circle with radius equal to 1.5µm. This conversion results in gap size threshold of 1963 pixels. The number of gaps formed that were larger

than 3µm in diameter due to exposure to Jurkat cells is seen in Figure 3.7 and the results of exposure to THP-1 cells are seen in Figure 3.8.

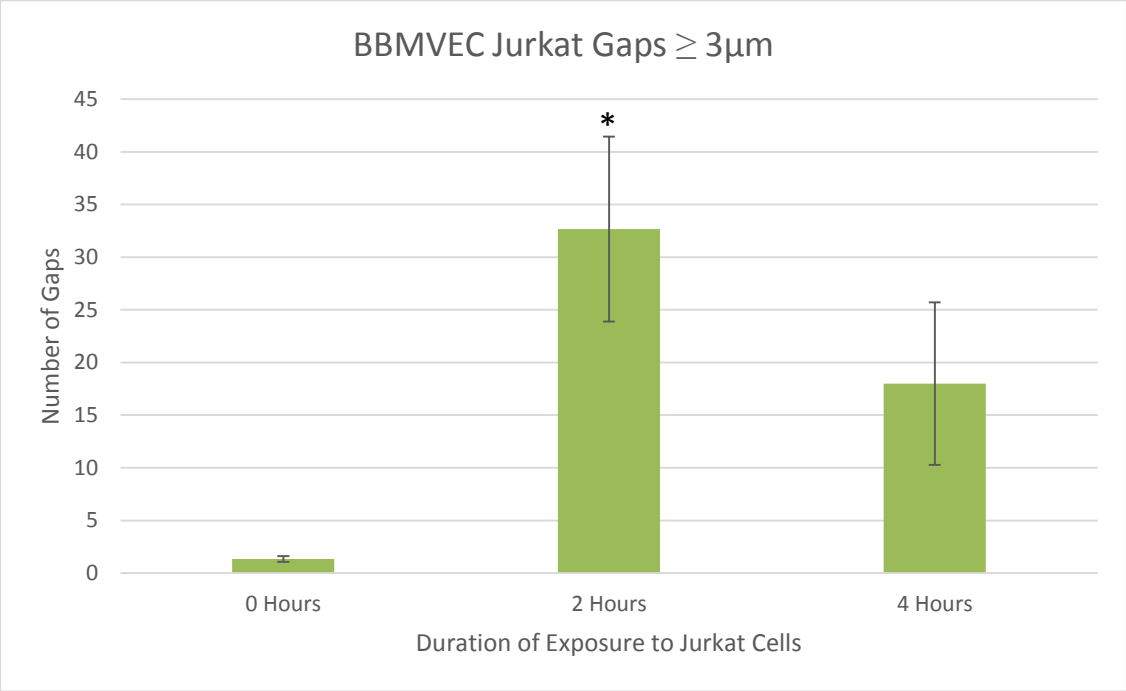

Figure 3.7 Number of gaps formed that were larger than 3µm in diameter on BBMVEC monolayer due to exposure to Jurkat cells. * indicated $p < 0.05$ with respect to 0 Hours. All values represent mean ± SEM for n = 3.

Results show that at 2 hours, the average number of gaps specifically larger than 3µm is at a maximum of 32.7. At 4 hours, the average number of gaps above this threshold of 3µm is 18. The 2-hour group is statistically significant compared to the no exposure group at a significance level of 95%.

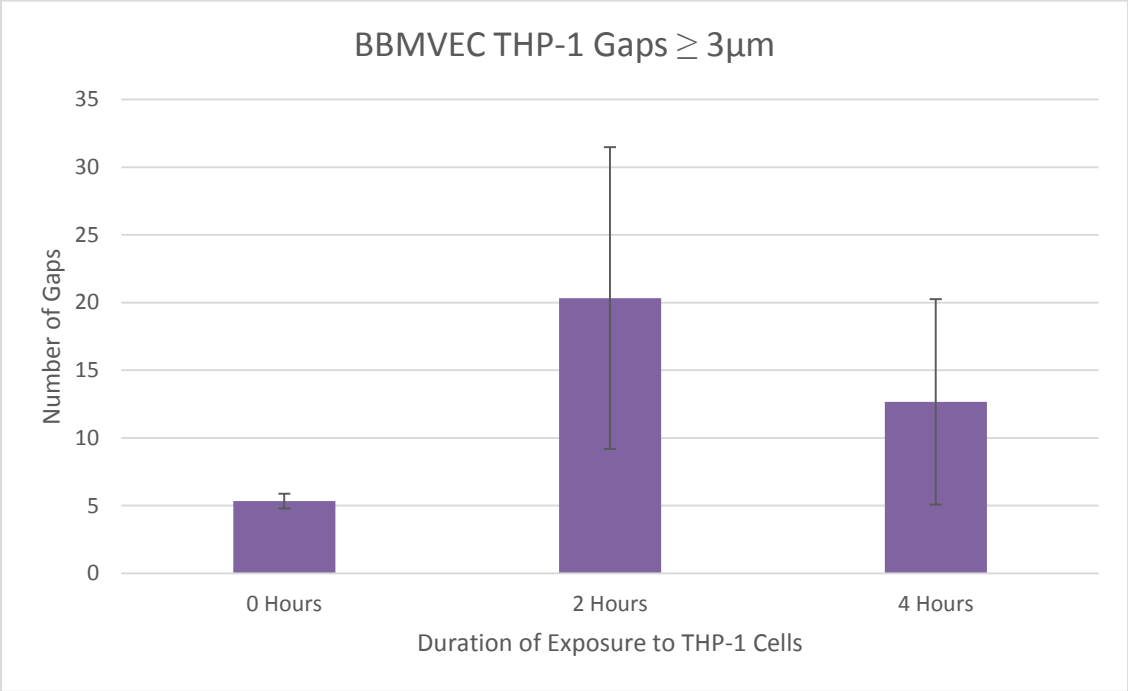

Figure 3.8 Number of gaps formed that were larger than 3µm in diameter on BBMVEC monolayer due to exposure to THP-1 cells. One-way ANOVA showed that the number of gaps greater than or equal to 3µm is not significant with regards to time where $p > 0.05$. All values represent mean ± SEM for $n = 3$.

For the BBMVEC THP-1 co-culture, the average number of gaps specifically larger than 3µm is at a maximum of 20.3 at 2 hours. At 4 hours, the average number of gaps above this threshold of 3µm is 12.7. Unlike the Jurkat cells, the THP-1 cells did not induce any significantly different number of gaps.

Figure 3.9 below compares the number gaps formed greater than 3µm between the Jurkat and THP-1 cells. The difference between Jurkat and THP-1 cells at each time point is not significant. However, each cell line shows a similar trend of greatest number of gaps formed at the 2-hour time point, and then a smaller amount remaining at 4 hours. Jurkat cells formed a greater number of gaps in the BBMVEC endothelium compared to the THP-1 cells at each time point.

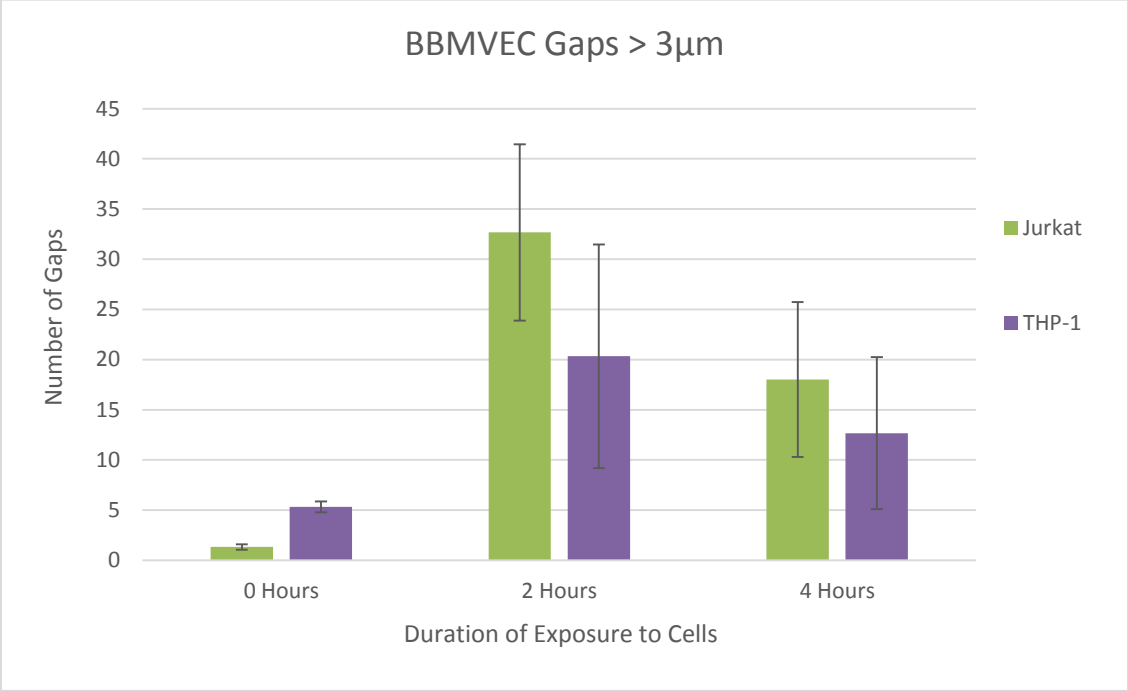

Figure 3.9 Comparison of number of gaps formed that were larger than 3µm in diameter on BBMVEC monolayer due to exposure to Jurkat and THP-1 cells individually. One-way ANOVA showed that the number of gaps greater than or equal to 3µm did not differ significantly at each time point based on the type of leukocyte where $p > 0.05$. All values represent mean ± SEM for $n = 3$.

3.2 Cytokine Mediated Disassembly via TNFα and THP-1 or Jurkat

Since cell-mediated drug delivery is meant to deliver drugs to the tumor, we decided to explore the gap formation of the endothelium during a state that represents the inflammation at the tumor microenvironment. To simulate inflammation, recombinant TNFα was added to the endothelium for several different exposure times. TNFα is a common cytokine present in inflammatory tissue and is often used to cause endothelial

cells to express cell adhesion molecules such as ICAM-1 and VCAM-1. In the following experiments, TNFα was added at 100U/mL.

In Figure 3.11, TNFα was added to the endothelium for 24 hours, removed, and then replaced with either fresh media (TNFα case) or fresh media containing the cells of interest (TNFα + Jurkat and TNFα + THP-1) and was left to culture for another 24 hours. 'Alone' represents no exposure to either TNFα or cells. Thus, the BBMVEC monolayer was examined after a total of 48 hours where the first 24 hours was a "stimulation period" of exposure to TNFα and the second 24 hours was free of TNFα.

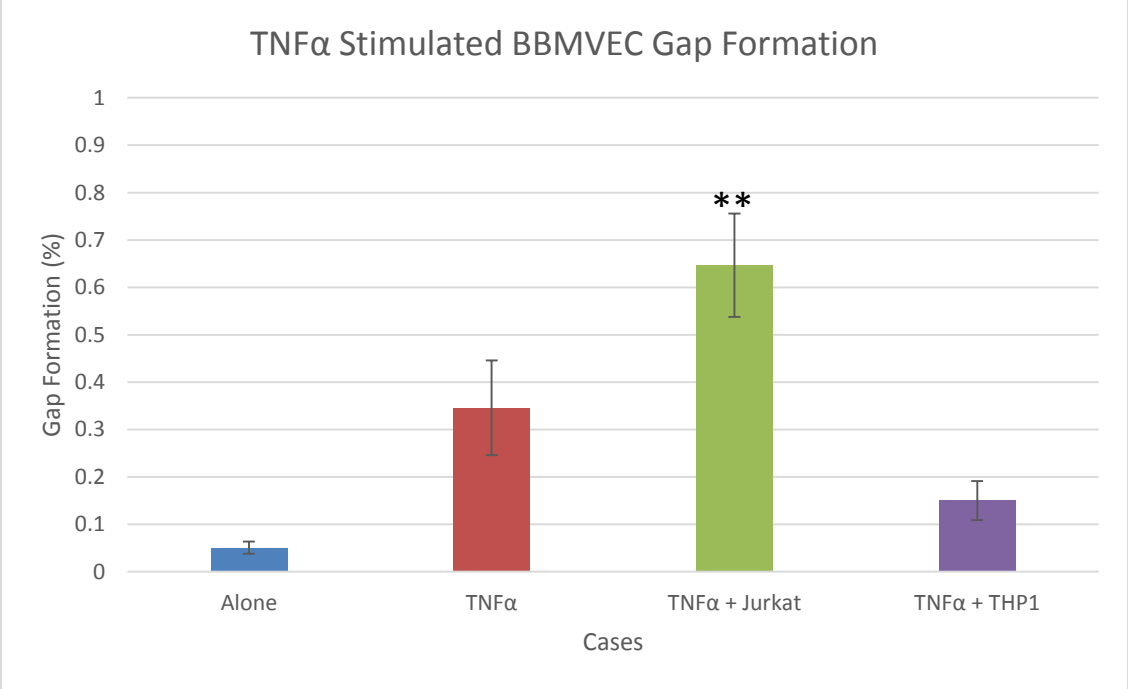

Figure 3.10 BBMVEC stimulated for 24 hours with TNFα then taken out of the culture media resulted in a significantly different gap formation when Jurkat cells were present in the media for the next 24 hours. Alone – no TNFα or cells; TNFα - BBMVEC stimulated for 24 hours with TNFα at 100U/mL then removed after 24 hours and replaced with fresh media; TNFα + Jurkat – BBMVEC stimulated for 24 hours with TNFα then removed and replaced with Jurkat cells in fresh media and cultured for another 24 hours; TNFα + THP1 – BBMVEC stimulated for 24 hours with TNFα then removed and replaced with THP-1 cells in fresh media and cultured for another 24 hours; values represented as means ± SEM for $n \geq 3$; ** indicated $p < 0.01$ with respect to 'Alone' and 'TNFα + THP-1'

Compared to the ‘Alone’ case of 0.05 % where no TNFα was added, the ‘TNFα’ group showed increased gap formation of 0.34 %, however it was not statistically different. BBMVEC co-culture with Jurkat cells after TNFα exposure had 0.65 % gap formation which is statistically significant from the ‘Alone’ group and the co-culture with THP-1 cells which only had 0.15 % gap formation.

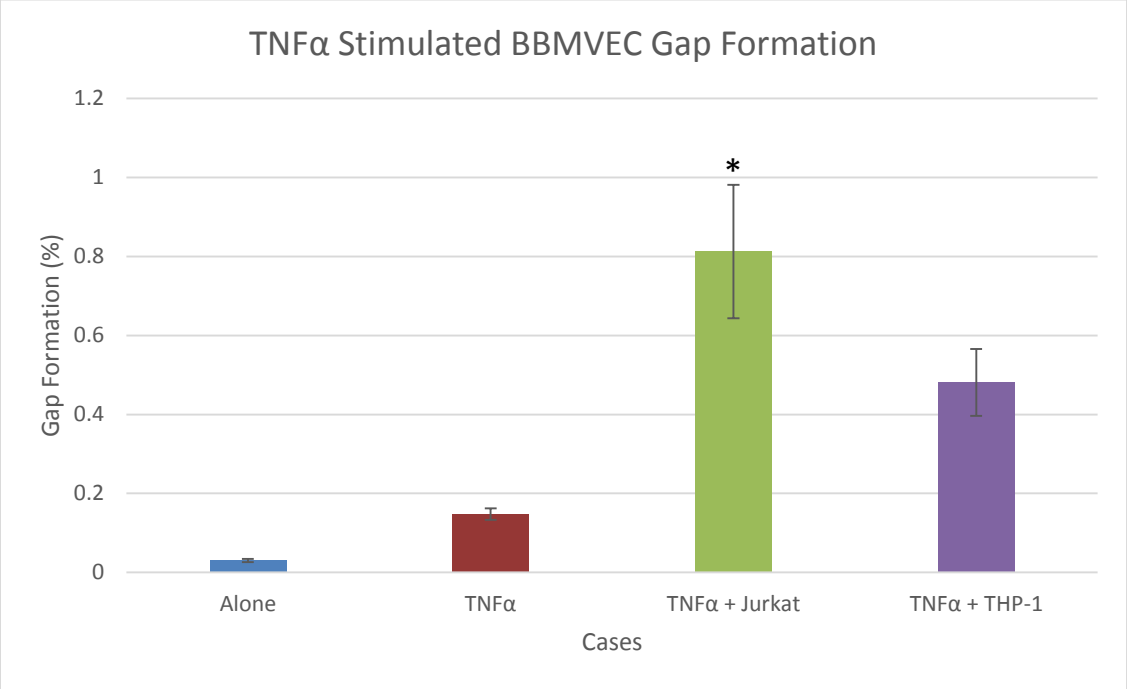

Figure 3.11 BBMVEC stimulated for 24 hours with TNFα and Jurkat cells together resulted in a significantly different gap formation when Jurkat cells were present in the media for the next 24 hours compared to the Negative and TNFα only group. Alone – no TNFα or cells; TNFα - BBMVEC stimulated for 24 hours with TNFα at 100U/mL then removed after 24 hours and replaced with fresh media; TNFα + Jurkat – BBMVEC stimulated for 24 hours with TNFα then removed and replaced with Jurkat cells in fresh media and cultured for another 24 hours; TNFα + THP1 – BBMVEC stimulated for 24 hours with TNFα then removed and replaced with THP-1 cells in fresh media and cultured for another 24 hours; values represented as means ± SEM for $n \geq 3$; * indicated $p < 0.05$ with respect to ‘Alone’ and ‘TNFα’

The results depicted in Figure 3.12 represent gap formation that was due to TNFα exposure for 24 hours by itself and with the presence of Jurkat or THP-1 cells for the same time frame. Therefore, this set of results represents the gap formation immediately

after the 24 hours of TNFα exposure. ‘Alone’ had minimal gap formation of 0.03 %, ‘TNFα’ had an average gap percentage of 0.15, ‘TNFα + Jurkat’ had an average gap percentage of 0.81, and ‘TNF + THP-1’ had an average gap formation of 0.48 %. The ‘TNFα + Jurkat’ group was statistically different from the ‘Alone’ and ‘TNFα’ groups.

Finally, the effect of 48-hour exposure to TNFα and the immune cells were studied. ‘Alone’ had the BBMVEC monolayer with no TNFα or immune cells added, and ‘TNFα’ had TNFα added to the culture medium for 48 hours. For ‘TNFα + Jurkat’ and ‘TNFα + THP-1’, the BBMVEC monolayer was exposed to TNFα for 24 hours, then the respective immune cells were added to the culture medium and allowed to culture for another 24 hours with TNFα remaining in the solution as well. The results are depicted in

Figure 3.13 below. There was no significant difference for when the cells were cultured in the presence of TNFα.

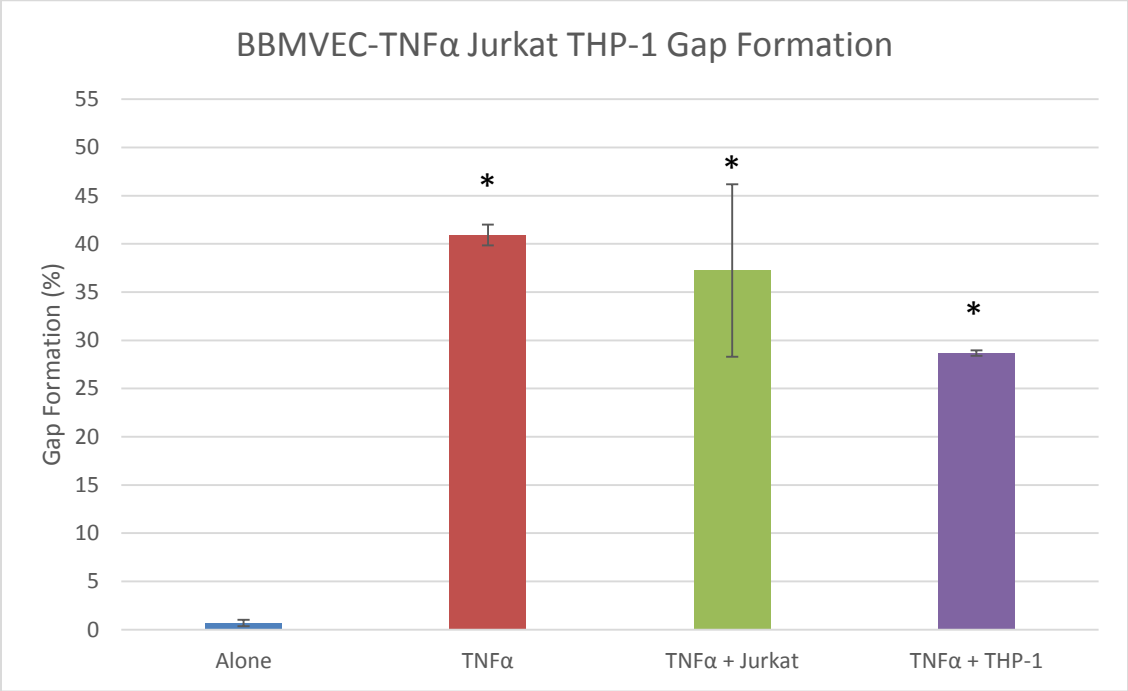

Figure 3.12 BBMVEC stimulated for 48 hours with TNFα alone, with TNFα and Jurkat cells together, and with TNFα and THP-1 cells together all resulted in a significantly different gap formation compared to the BBMVEC alone. Alone – no TNFα or cells; TNFα - BBMVEC stimulated for 48 hours with TNFa at 100U/mL; TNFα + Jurkat – BBMVEC stimulated for 24 hours with TNFα then removed and replaced with Jurkat cells in media containing TNFα at 100U/mL for another 24 hours; TNFα + THP1 – BBMVEC stimulated for 24 hours with TNFα then removed and replaced with THP-1 cells in media containing TNFα at 100U/mL and cultured for another 24 hours; values represented as means ± SEM for n = 3; * indicated $p<0.05$ with respect to 'Alone'

3.3 Endothelial – Human WBCs Co-Culture

The studies were expanded to examine how the BBMVEC monolayer reacts to co-culture with human WBCs. WBCs is all types of white blood cells, so the sample included monocytes, neutrophils, lymphocytes, eosinophils, and basophils from a healthy volunteer. Results are seen below in Figure 3.14.

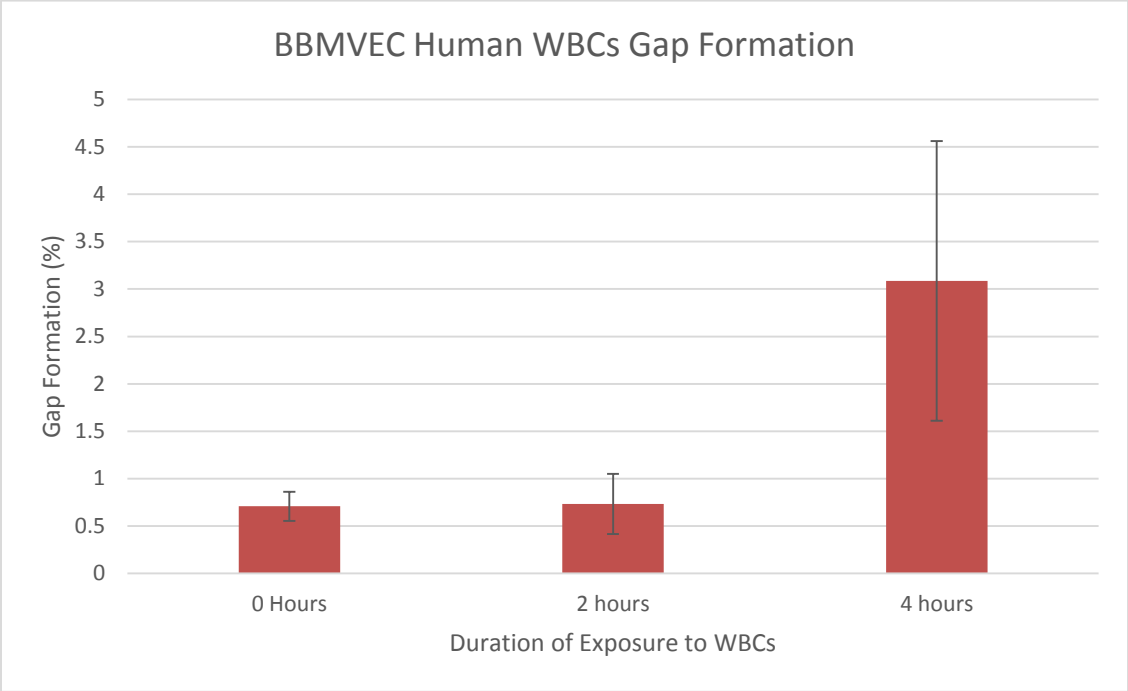

Figure 3.13 Co-culture between BBMVEC and WBCs does not produce significant gap formation. 0 Hours – no WBCs added; 2 hours – WBCs added for 2 hours in co-culture with BBMVEC; 4 hours – WBCs added for 4 hours in co-culture with BBMVEC. One-way ANOVA showed that the gap formation between the cases were not significant for all time points and the p-value > 0.05. Values represent means ± SEM for n = 3

The 'Alone' group which was not exposed to any WBCs showed the least gap formation with an average of 0.71 %. Next was the 2-hour time point with a minimal increase to 0.73 % gap formation. Finally, the 4-hour time point had the largest gap formation with 3.09 % gap formation. However, a large error for this time point results in this value not being significant at the 95 % confidence level.

Figure 3.15, seen below, compares the gap formation percentage between the WBCs and the previously depicted gap formation percentages due to Jurkat and THP-1 cells. The decreasing gap formation percentage is seen again in the Jurkat and THP-1 cases, but the WBC case increases with time. The highest percentage of gap formation in

these cases is the 2-hour group for Jurkat co-culture. Yet, the differences within each time point for each type of immune cell were not significant.

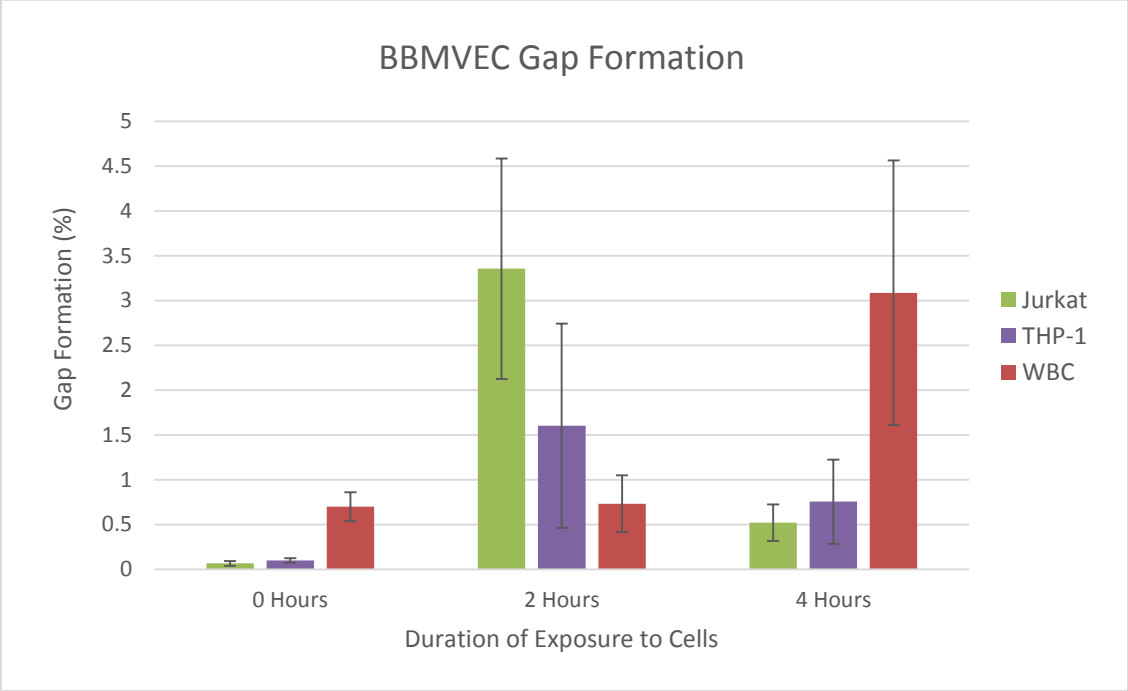

Figure 3.14 Comparison of gap formation percentage due to Jurkat, THP-1, and whole WBCs for matching time points. Negative represents a case with no exposure to Jurkat, THP-1 or WBCs. One-way ANOVA showed that the gap formation between the cases were not significant for all time points and the p-value > 0.05. Values are means ± SEM for n = 3

3.4 Chemotaxis of THP-1 and Jurkat

To help develop the model for cell-mediated drug delivery, a chemotaxis study was conducted for the two main cell lines used throughout this study to see how they would migrate from the blood flow to the tumor microenviroment. A 48-well Boyden chamber was used to perform the chemotaxis study. The chemoattractant MCP1 was used at a concentration of 100ng/mL for all cases except ‘Alone’ where no chemoattractant was placed in the bottom well. The ‘2 hours’ and ‘4 hours’ cases represent THP-1 and

Jurkat migration for 2 hours and 4 hours respectively. Results are seen below in Figure 3.16.

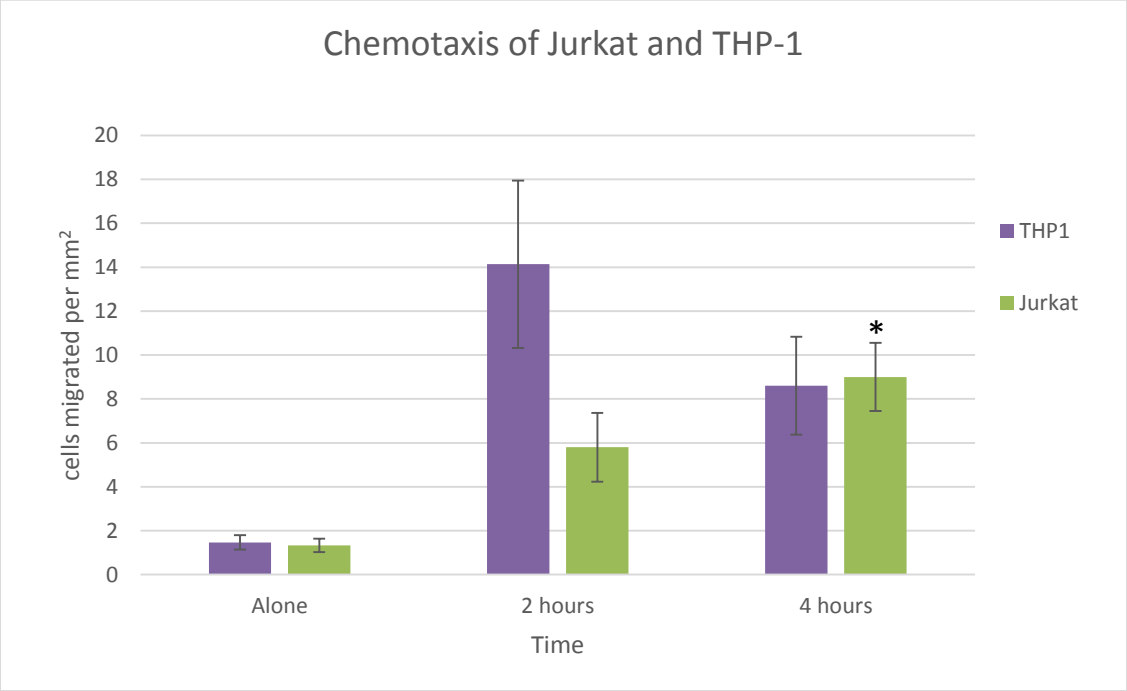

Figure 3.15 Jurkat cells migrated to MCP1 after 4 hours. Alone – no MCP1 added in bottom well of Boyden chamber; 2 hours – THP-1 or Jurkat cells added to top well of Boyden Chamber and were allowed to migrate for 2 hours to the bottom chamber; 4 hours - THP-1 or Jurkat cells added to top well of Boyden Chamber and were allowed to migrate for 4 hours to the bottom chamber; values represented as means ± SEM for n = 3; * indicated $p < 0.05$ with respect to 'Alone'

Results show that Jurkat cells that were allowed to migrate for 4 hours was the only case of significant difference in terms of migration in response to the chemoattractant MCP1. Without any chemoattractant, an average of 1.33 Jurkat cells and 1.47 THP-1 cells per mm^2 migrated through the filter, as seen in the 'Alone' column. At 2 hours, an average of 5.80 and 14.13 cells per mm^2 migrated for Jurkat and THP-1 cells, respectively. For the 4-hour mark, an average of 9 Jurkat cells and 8.6 THP-1 cells per mm^2 migrated as a result of the presence of MCP1. While it is not significant, the number

of THP-1 cells that migrated in 2 hours is the highest average number of cells migrated per mm^2 in this study.

Chapter 4

Discussion

Transendothelial migration is the biological process of leukocytes crossing the endothelium to enter diseased tissue. This process is regulated by adherens junctions and, because VE-cadherin is one of the most prominent adherens junction proteins, it is an important regulator of transendothelial migration (Allingham et al., 2007). Jurkat cells are a lymphocyte-like cell line that constitutively express VLA-4, the counter-receptor for VCAM-1 (Ricard et al., 1997). THP-1 cells are a monocyte-like cell line that constitutively express LFA-1 which is one of the counter-receptors for ICAM-1 (Marlin and Springer, 1987; Mittar et al., 2011). Our lab has previously shown that the VE-cadherin disassembly is partially mediated by VCAM-1 binding events on Human Umbilical Vein Endothelial Cells (HUVECs) instead of BBMVEC (Khanna et al., 2010). Also, other groups have shown through different experimental methods that ICAM-1 binding events leads to tyrosine phosphorylation of VE-cadherin, which is a crucial step in its disassembly and plays a role in the transendothelial migration of monocytes (Allingham et al., 2007; Dejana et al., 2008). The work done in this thesis is meant to help construct a model for cell-mediated drug delivery through the blood-brain barrier and understand the dynamics of the blood-brain barrier.

4.1 Analysis of Endothelial Gap Formation Due to Leukocyte Co-Culture

When all time points are considered as one group with the Jurkat or THP-1 cells being cultured on a BBMVEC monolayer, there is a significant gap formation when the endothelium is cultured with Jurkat cells, but no significant gap formation with THP-1 cells. However, when each time point is considered on its own, the gap formation percentages did not have a significant difference as a function of time on a large scale. However, it appears that if any gap formation were to occur due to the solitary presence of a particular type of white blood cell, it would occur within the 2-hour time frame where gap formation was the highest for both types of white blood cells. For both cell lines, the percent gap formation in the BBMVEC cells decreased with time. It is important to note that when comparing the percent gap formation between Jurkat cells and the THP-1 cells at each of their time points, the Jurkat cells have a higher gap formation percentage than the THP-1 cells at all time points except the 4-hour point, yet the difference is not significant for any of the time points. Regardless, this response between the immune cells and the BBMVEC monolayer must play a role in determining which cell line is more appropriate for the use of cell-mediated drug delivery.

To further characterize the gap formation, the number of gaps that were formed, as opposed to the percentage due to area, was calculated. Assuming that the gaps are circular, a 3μm diameter gap was used as a threshold to verify this model in terms of transendothelial migration, since migration will typically not occur in gaps less than 3μm (Smith et al., 1991). Results showed similar results to the lumped gap formation analysis where the Jurkat cells showed a significantly more number of gaps at the 2-hour time

point. THP-1 cells did not induce a significantly more number of gaps greater than 3μm compared to the control or based on the time points of 2 hours and 4 hours. Important to developing this model, the Jurkat cells formed more gaps than THP-1 cells at both time points, however this difference was not significant.

The significant gap formation from the presence of Jurkat cells on the BBMVEC endothelium in the case of all time points considered and with number of gaps greater than 3μm in diameter is most likely due to the interaction between endothelial cellular adhesion molecules, VCAM-1 or ICAM-1, that bind to VLA-4 and LFA-1, respectively (Elices et al., 1990; Lawrence and Springer, 1991). However, gap formation percentages are very low in both cases of exposure to either Jurkat cells or THP-1 cells, so this must be looked into further to determine that there is a sufficient amount of signaling between the integrins and cellular adhesion molecules of the participating cell types. In this case of experiments, the endothelium was not activated, an event typical of inflammation that leads to increased VE-cadherin disassembly and leukocyte transendothelial migration (Muller, 2009). While gap formation is not a direct indication of increased ability to transmigrate through the endothelium, it does indicate the presence of the signaling event that leads to VE-cadherin disassembly. This disassembly is required for transmigration through the endothelium, at least via the paracellular route (Dejana et al., 2008).

4.2 Analysis of Cytokine Mediated Disassembly via TNFα and THP-1 or Jurkat

Since gap formation occurs most often in a state of inflammation that induces upregulation of surface marker expression, the activation of the endothelial layer was explored to determine if gap formation would increase due to VLA-4/VCAM-1 or LFA-1/ICAM-1 interactions. To accomplish this, BBMVEC cells were cultured in the presence of TNFα and for different lengths of time to examine its potential transient effect on gap formation. We showed that 24-hour exposure to TNFα and then subsequent removal of the TNFα only resulted in a significant increase in gap formation in the presence of Jurkat cells compared to the case where no TNFα was added at all and the case where THP-1 cells were added to the BBMVEC cells after TNFα stimulation. In this scenario, VCAM-1 may be expressed at low levels due to the initial TNFα exposure and then decreases slightly with the additional culture of 24 hours without the TNFα, yet it proved to be enough for the VCAM-1/VLA-4 mediated gap formation. Since there was no significant gap formation from the TNFα + THP-1 group, the question of whether or not ICAM-1 is upregulated by the presence of TNFα for BBMVECs arises.

The scenario of inflammatory activation of the endothelium was examined further by culturing the BBMVEC monolayer with TNFα for 24 hours again, but having the Jurkat and THP-1 cells accompany the TNFα for the full 24 hours. Interestingly enough, this case did not result in a large amount of gap formation. Granted, gap formation was statistically significant for the TNFα stimulated monolayer cultured with the Jurkat cells, this time compared to the TNFα only control and the control without TNFα as well. In

this situation, it appears that the presence of a large amount of lymphocytes could encourage increased gap formation in the endothelium (via the VCAM-1/VLA-4 pathway) and the resulting breakdown of VE-cadherin would allow a greater number of immune cells to enter the tissue. In the context of cell-mediated drug delivery, this would result in a more efficient delivery of therapeutics via lymphocytes compared the monocytes.

Gap formation was the largest when the endothelium was cultured with the TNFα for a full consecutive 48 hours. The extent to gap formation was so large that the TNFα only group experienced the most gap formation, while the groups that also had Jurkat cells and THP-1 cells actually had gap formation percentages less than that of the TNFα only. It appears that at a certain point, the damage done by the inflammatory cytokines is so great, in terms endothelial permeability, that any potential upregulation of surface molecule expression on the remaining endothelial cells would not have participated in enough binding for the THP-1 or Jurkat cells to bind to and launch the signaling network that leads to increased VE-cadherin disassembly.

4.3 Analysis of Preliminary Results of Human WBCs with the BBMVEC Monolayer

The gap studies were continued such that WBCs from a human were tested with the BBMVEC monolayer in order to determine if the presence of multiple types of leukocytes would achieve greater gap formation. What we learned from this experiment is that freshly harvested WBCs will not cause a significant increase in endothelial gaps,

just as the individual Jurkat and THP-1 cultures would not. For this study the time point of 8 hours were not examined. So, there is the possibility that when dealing with human cells, endothelial gap formation increases with time since the 4-hour time point has the highest gap formation when compared to the case with no WBCs and the WBCs in co-culture for only 2 hours. This did not follow the trend that was seen with the Jurkat and THP-1 cells in co-culture with the BBMVEC monolayer. If this were the case, the reasons could range from the fact that the WBCs had the ability to interact with all the other types of WBCs and therefore a different type of reaction was occurring that delayed the gap formation when compared with the Jurkat or THP-1 cases. This may have also been the result of cooperative effects of lymphocytes and monocytes working together in the same culture environment. Future studies should look at how a co-culture between THP-1 and Jurkat cells on a BBMVEC endothelium compare with this whole WBC on BBMVEC endothelium case. The difference between the 4-hour time point, the 2-hour time point, and the control were not significant, so this trend is not a guarantee either, and suggests that this accurately represents a non-inflammatory environment. Another reason for the lack of significant gap formation could be the species incompatibility of bovine endothelial cells with human WBCs.

4.4 Analysis of Jurkat and THP-1 Chemotaxis

The chemotactic ability of the white blood cell lines is important in the development of a cell-mediated drug delivery model. The Jurkat cells proved to migrate the most as seen in its 4-hour time point. THP-1 had an increased migration when

exposed to the chemoattractant MCP1, proving that it has the ability to migrate through a filter, yet neither of the time points had a statistically significant increase in the number of cells that migrated. The average number of THP-1 cells that migrated was unexpectedly not statistically significant, given that MCP-1 is monocyte chemotactic protein – 1. Other studies have shown that migration of THP-1 at 100ng/mL of MCP-1 to be less than migration at lower concentrations of chemoattractant (Kito and Nishida, 2002). However from this scenario, Jurkat cells would thus prove to be a promising carrier for drugs that are to be delivered via cell-mediated drug delivery. The 8μm pores are much larger than the 3μm threshold that was being examined in the gap number studies, therefore this should be repeated with smaller pore sizes.

Chapter 5

Conclusions and Future Work

Gap formation in a BBMVEC model of the BBB endothelium is not easily achieved. Jurkat cells were both able to create a significant gap formation in the BBMVEC monolayer when all time points were considered together as an exposure group versus no exposure to cells. THP-1 cells were not able to induce significant gap formation though. Looking at the distribution of the gap percentage with time, both Jurkat and THP-1 cells induced greatest percentage of gap formation and number of gaps formed at 2 hours. The time course study further indicated that gap formation appears to decrease with time and that the greatest gap formation may form at some time point within 2 hours. Furthermore, human white blood cells were not able to create any significant gap formation in the BBMVEC monolayer, but gap formation increased with time, in contrast to cases with Jurkat or THP-1 cells. BBMVECs did not retain cellular adhesion molecule expression over a 24-hour period after being stimulated with TNFα for an initial 24-hour period which resulted in minimal gap formation via VCAM-1/VLA-4 and ICAM-1/LFA-1 or possibly ICAM-1/Mac-1 pathways. Gap formation increased slightly when immediately measured after 24 hours of TNFα exposure when in co-culture with Jurkat cells but not with THP-1 cells. Finally, Jurkat and THP-1 cells were tested for their ability to migrate towards a chemoattractant through an 8μm filter. Four hours of migration time allowed a significant number of Jurkat cells to migrate through the filter compared to the lower time points and migration of THP-1 under the same conditions.

These results put together lay the foundation for a lot of work to be done in field of cell-mediated drug delivery through the BBB. Future work can be done in relation to several of the experiments conducted for the completion of this thesis. The trend of decreasing gap formation with increased time between the BBMVEC and the Jurkat and THP-1 cells suggests that perhaps lower time points should be explored where there may be even high gap formation percentage. Furthermore, gap formation in BBMVEC co-cultured with a mixture of THP-1 and Jurkat cells can be studied as one case with respect to time. Additional studies should be done that look at the gap formation of BBMVEC with WBCs at higher and lower time points, as well as repeating the ones already run to confirm this trend in increasing gap formation with time.

In terms of the stimulated endothelium studies, they should be repeated to confirm that the extreme change in gap formation between 24 hours of TNFα exposure and 48 hours of TNFα exposure is the correct biological response. However, if the results are similar to the ones presented here, then an intermediate time point of 36 hours should be tested to see if the change in gap formation follows that steep trend. To confirm the role of VLA-4/VCAM-1 on increased gap formation compared with LFA-1/ICAM-1, blocking studies should be run with VLA-4 on the Jurkat cells and a lower gap formation would confirm the results presented in this thesis. Additionally, 24 hours of co-culture with the Jurkat or THP-1 cells were too long and this should be accounted for in the cytokine mediated disassembly studies with future experiments calculating gap formation percentage at 2 hours, at the most, after TNFα stimulation.

Finally, it also seems worthy to explore using a different cell line to represent the blood-brain barrier for this model. Using a bovine species blood-brain barrier cell line

does not portray the most realistic in vivo environment with regards to cell-mediated drug delivery for humans. Therefore, human blood-brain barrier cell lines should be tested to see if that species compatibility was an issue or not. Overall, Jurkat cells showed increased gap formation in multiple aspects (gap size and number) while also migrating significantly through a porous filter, and for now appears to be the best candidate for a leukocyte in this blood brain barrier model in terms of transendothelial migration.

Appendix

Table 1. % Gap Formation values THP-1 BBMVEC co-culture time course – Alone

		AVERAGE GAP FORMATION (%)
THP-1 ALONE TIME COURSE	Slide 1	0.084
	Slide 2	0.16
	Slide 3	0.056

Table 2. % Gap Formation values THP-1 BBMVEC co-culture time course – 2 Hours

		AVERAGE GAP FORMATION (%)
THP-1 2 HOURS TIME COURSE	Slide 1	0.282
	Slide 2	0.133
	Slide 3	4.39

Table 3. % Gap Formation values THP-1 BBMVEC co-culture time course – 4 Hours

		AVERAGE GAP FORMATION (%)
THP-1 4 HOURS TIME COURSE	Slide 1	0.336
	Slide 2	1.89
	Slide 3	0.038

Table 4. % Gap Formation values THP-1 BBMVEC co-culture time course – 8 Hours

		AVERAGE GAP FORMATION (%)
THP-1 8 HOURS TIME COURSE	Slide 1	0.456
	Slide 2	0.251
	Slide 3	1.05

Table 5. % Gap Formation values Jurkat BBMVEC co-culture time course – Alone

		AVERAGE GAP FORMATION (%)
JURKAT ALONE TIME COURSE	Slide 1	0.133
	Slide 2	0.038
	Slide 3	0.032

Table 6. % Gap Formation values Jurkat BBMVEC co-culture time course – 2 Hours

		AVERAGE GAP FORMATION (%)
JURKAT 2 HOURS TIME COURSE	Slide 1	0.393
	Slide 2	4.36
	Slide 3	5.31

Table 7. % Gap Formation values Jurkat BBMVEC co-culture time course – 4 Hours

		AVERAGE GAP FORMATION (%)
JURKAT 4 HOURS TIME COURSE	Slide 1	0.121
	Slide 2	0.978
	Slide 3	0.459

Table 8. % Gap Formation values Jurkat BBMVEC co-culture time course – 8 Hours

		AVERAGE GAP FORMATION (%)
JURKAT 8 HOURS TIME COURSE	Slide 1	1.04
	Slide 2	0.657
	Slide 3	0.344

Table 9. Number of Gaps > 3µm THP-1 – Alone

		NUMBER OF GAPS
THP-1 ALONE	Slide 1	6
	Slide 2	6
	Slide 3	4

Table 10. Number of Gaps > 3µm THP-1 – 2 Hours

		NUMBER OF GAPS
THP-1 2 HOURS	Slide 1	12
	Slide 2	2
	Slide 3	47

Table 11. Number of Gaps > 3µm THP-1 – 4 Hours

		NUMBER OF GAPS
THP-1 4 HOURS	Slide 1	6
	Slide 2	31
	Slide 3	1

Table 12. Number of Gaps > 3µm Jurkat - Alone

		NUMBER OF GAPS
JURKAT ALONE	Slide 1	2
	Slide 2	1
	Slide 3	1

Table 13. Number of Gaps > 3µm Jurkat – 2 Hours

		NUMBER OF GAPS
JURKAT 2 HOURS	Slide 1	13
	Slide 2	35
	Slide 3	50

Table 14. Number of Gaps > 3µm Jurkat – 4 Hours

		NUMBER OF GAPS
JURKAT 4 HOURS	Slide 1	4
	Slide 2	36
	Slide 3	14

Table 15. % Gap Formation for Cytokine Mediated Disassembly (24 hours on 24 hours off) – Alone

		AVERAGE GAP FORMATION (%)
	Slide 1	0.022

CYTOKINE MEDIATED DISASSEMBLY - (THP-1 GROUP) ALONE	Slide 2	0.039
	Slide 3	0.038

Table 16. % Gap Formation for Cytokine Mediated Disassembly (24 hours on 24 hours off) – TNFα

		AVERAGE GAP FORMATION (%)
CYTOKINE MEDIATED DISASSEMBLY - (THP-1 GROUP) TNFα (24 ON 24 OFF)	Slide 1	0.07
	Slide 2	0.74
	Slide 3	0.094

Table 17. % Gap Formation for Cytokine Mediated Disassembly (24 hours on 24 hours off) – TNFα + THP-1

		AVERAGE GAP FORMATION (%)
TNFα + THP-1 (24 ON 24 OFF)	Slide 1	0.089
	Slide 2	0.25
	Slide 3	0.111

Table 18. % Gap Formation for Cytokine Mediated Disassembly (24 hours on 24 hours off) – Alone

		AVERAGE GAP FORMATION (%)
CYTOKINE MEDIATED DISASSEMBLY - (JURKAT GROUP) ALONE	Slide 1	0.02
	Slide 2	0.08
	Slide 3	0.106

Table 19. % Gap Formation for Cytokine Mediated Disassembly (24 hours on 24 hours off) – TNFα

AVERAGE GAP FORMATION (%)

CYTOKINE MEDIATED DISASSEMBLY - (JURKAT GROUP) TNFα (24 HOURS ON 24 HOURS OFF)	Slide 1	0.257
	Slide 2	0.332
	Slide 3	0.582

Table 20. % Gap Formation for Cytokine Mediated Disassembly (24 hours on 24 hours off) – TNFα + Jurkat

	AVERAGE GAP FORMATION (%)	
CYTOKINE MEDIATED DISASSEMBLY - TNFα + JURKAT (24 HOURS ON 24 HOURS OFF)	Slide 1	0.737
	Slide 2	0.819
	Slide 3	0.384

Table 21. % Gap Formation for Cytokine Mediated Disassembly (24 hours) – Alone

	AVERAGE GAP FORMATION (%)	
CYTOKINE MEDIATED DISASSEMBLY - ALONE (24 HR)	Slide 1	0.033
	Slide 2	0.036
	Slide 3	0.021

Table 22. % Gap Formation for Cytokine Mediated Disassembly (24 hours) – TNFα

	AVERAGE GAP FORMATION (%)	
CYTOKINE MEDIATED DISASSEMBLY - TNFα (24 HR)	Slide 1	0.136
	Slide 2	0.124
	Slide 3	0.183

Table 23. % Gap Formation for Cytokine Mediated Disassembly (24 hours) – TNFα + THP-1

	AVERAGE GAP FORMATION (%)	
CYTOKINE MEDIATED	Slide 1	0.432

DISASSEMBLY - TNFα + THP-1 (24 HR)	Slide 2	0.331
	Slide 3	0.680

Table 24. % Gap Formation for Cytokine Mediated Disassembly (24 hours) – TNFα + Jurkat

		AVERAGE GAP FORMATION (%)
CYTOKINE MEDIATED DISASSEMBLY - TNFα + JURKAT (24 HR)	Slide 1	0.962
	Slide 2	1.07
	Slide 3	0.404

Table 25. % Gap Formation for Cytokine Mediated Disassembly (48 hours) – Alone

		AVERAGE GAP FORMATION (%)
CYTOKINE MEDIATED DISASSEMBLY - ALONE (48 HOURS)	Slide 1	1.51
	Slide 2	0.433
	Slide 3	0.135

Table 26. % Gap Formation for Cytokine Mediated Disassembly (48 hours) – TNFα

		AVERAGE GAP FORMATION (%)
CYTOKINE MEDIATED DISASSEMBLY – (THP-1 GROUP) TNFα (48 HOURS)	Slide 1	42.8
	Slide 2	41.7
	Slide 3	38.4

Table 27. % Gap Formation for Cytokine Mediated Disassembly (48 hours) – TNFα + THP-1

		AVERAGE GAP FORMATION (%)
CYTOKINE MEDIATED DISASSEMBLY -	Slide 1	28.4
	Slide 2	28.3

TNFA + THP1 (48 HOURS)	Slide 3	39.4

Table 28. % Gap Formation for Cytokine Mediated Disassembly (48 hours) – TNFα + Jurkat

		AVERAGE GAP FORMATION (%)
CYTOKINE MEDIATED DISASSEMBLY - TNFα + JURKAT (48 HOURS)	Slide 1	15.6
	Slide 2	45.1
	Slide 3	51.0

Table 29. THP-1 Chemotaxis Number of Cells Migrated

	THP-1								
	Control			2 hours			4 hours		
Sample	1	2	3	1	2	3	1	2	3
Number of Cells	2	1	1	3	6	17	11	3	11
	2	4	0	6	5	33	12	3	18
	3	0	1	32	20	10	6	3	15
	1	0	1	4	7	9	4	6	5
	3	2	1	7	5	48	0	11	21
AVERAGE	2.2	1.4	0.8	10.4	8.6	23.4	6.6	5.2	14

Table 30. Jurkat Chemotaxis Number of Cells Migrated

	Jurkat								
	Control			2 hours			4 hours		
Sample	1	2	3	1	2	3	1	2	3
Number of Cells	0	3	3	14	0	1	1	10	30
	1	0	2	7	4	9	9	18	5
	4	0	2	4	2	5	1	15	8
	2	0	1	6	6	0	2	3	5
	1	0	1	17	10	2	13	8	7
AVERAGE	1.6	0.6	1.8	9.6	4.4	3.4	5.2	10.8	11

Bibliography

Abbott, N. J. (2013). Blood-brain barrier structure and function and the challenges for CNS drug delivery. *J. Inherit. Metab. Dis.* **36**, 437–449.

Abbott, N. J., Rönnbäck, L. and Hansson, E. (2006). Astrocyte–endothelial interactions at the blood–brain barrier. *Nat. Rev. Neurosci.* **7**, 41–53.

Allingham, M. J., van Buul, J. D. and Burridge, K. (2007). ICAM-1-Mediated, Src- and Pyk2-Dependent Vascular Endothelial Cadherin Tyrosine Phosphorylation Is Required for Leukocyte Transendothelial Migration. *J. Immunol.* **179**, 4053–4064.

Bravi, L., Dejana, E. and Lampugnani, M. G. (2014). VE-cadherin at a glance. *Cell Tissue Res.* **355**, 515–522.

Butt, A. M., Jones, H. C. and Abbott, N. J. (1990). Electrical resistance across the blood-brain barrier in anaesthetized rats: a developmental study. *J. Physiol.* **429**, 47–62.

Cavallo, F., De Giovanni, C., Nanni, P., Forni, G. and Lollini, P. L. (2011). 2011: The immune hallmarks of cancer. *Cancer Immunol. Immunother.* **60**, 319–326.

Chambers, A. F., Groom, A. C. and MacDonald, I. C. (2002). Dissemination and growth of cancer cells in metastatic sites. *Nat. Rev. Cancer* **2**, 563–72.

Chen, Y. and Liu, L. (2012). Modern methods for delivery of drugs across the blood-brain barrier. *Adv. Drug Deliv. Rev.* **64**, 640–665.

Chertok, B., Moffat, B. A., David, A. E., Yu, F., Bergemann, C., Ross, B. D. and Yang, V. C. (2008). Iron oxide nanoparticles as a drug delivery vehicle for MRI monitored magnetic targeting of brain tumors. *Biomaterials* **29**, 487–496.

Cserr, H. F. and Bundgaard, M. (1984). Blood-brain interfaces in vertebrates: a comparative approach. *Am. J. Physiol.* **246**, R277–R288.

Dejana, E., Orsenigo, F. and Lampugnani, M. G. (2008). The role of adherens junctions and

VE-cadherin in the control of vascular permeability. *J. Cell Sci.* **121**, 2115–2122.

Diamond, M. S., Staunton, D. E., De Fougerolles, A. R., Stacker, S. A., Garcia-Aguilar, J., Hibbs, M. L. and Springer, T. A. (1990). ICAM-1 (CD54): A counter-receptor for Mac-1 (CD11b/CD18). *J. Cell Biol.* **111**, 3129–3139.

Ekeblad, S., Sundin, A., Janson, E. T., Welin, S., Granberg, D., Kindmark, H., Dunder, K., Kozlovacki, G., Orlefors, H., Sigurd, M., et al. (2007). Temozolomide as monotherapy is effective in treatment of advanced malignant neuroendocrine tumors. *Clin. Cancer Res.* **13**, 2986–2991.

Elices, M. J., Osborn, L., Takada, Y., Crouse, C., Luhowskyj, S., Hemler, M. E. and Lobb, R. R. (1990). VCAM-1 on activated endothelium interacts with the leukocyte integrin VLA-4 at a site distinct from the VLA-4/Fibronectin binding site. *Cell* **60**, 577–584.

Falk, W., Goodwin, R. H. and Leonard, E. J. (1980). A 48-well micro chemotaxis assembly for rapid and accurate measurement of leukocyte migration. *J. Immunol. Methods* **33**, 239–247.

Ingber, D. E. (1993). Cellular tensegrity: defining new rules of biological design that govern the cytoskeleton. *J. Cell Sci.* **104 (Pt 3**, 613–627.

Khanna, P., Yunkunis, T., Muddana, H. S., Peng, H. H., August, A. and Dong, C. (2010). p38 MAP kinase is necessary for melanoma-mediated regulation of VE-cadherin disassembly. *Am. J. Physiol. Cell Physiol.* **298**, C1140–50.

Kito, K. and Nishida, K. ichi (2002). Nonrequirement of continuous stimulation with MCP-1 for cell migration and determination of directional migration by initial stimulation with chemokine. *Exp. Cell Res.* **281**, 157–66.

Lawrence, M. B. and Springer, T. a. (1991). Leukocytes roll on a selectin at physiologic flow rates: distinction from and prerequisite for adhesion through integrins. *Cell* **65**, 859–873.

Ley, K., Laudanna, C., Cybulsky, M. I. and Nourshargh, S. (2007). Getting to the site of inflammation: the leukocyte adhesion cascade updated. *Nat. Rev. Immunol.* **7**, 678–89.

Machinable, L., Conductive, E. and Alc, T. (2010). • Invited Review. **26**, 385–416.

Marlin, S. D. and Springer, T. A. (1987). Purified intercellular adhesion molecule-1 (ICAM-1) is a ligand for lymphocyte function-associated antigen 1 (LFA-1). *Cell* **51**, 813–819.

Mittar, D., Paramban, R. and Mcintyre, C. (2011). Flow Cytometry and High-Content Imaging to Identify Markers of Monocyte-Macrophage Differentiation. *BD Biosci.* 20.

Muller, W. A. (2009). Mechanisms of transendothelial migration of leukocytes. *Circ. Res.* **105**, 223–230.

Muller, W. A., Weigl, S. A., Deng, X. and Phillips, D. M. (1993). PECAM-1 is required for transendothelial migration of leukocytes. *J. Exp. Med.* **178**, 449–60.

Navarro, P., Caveda, L., Breviario, F., M??ndoteanu, I., Lampugnani, M. G. and Dejana, E. (1995). Catenin-dependent and -independent functions of vascular endothelial cadherin. *J. Biol. Chem.* **270**, 30965–30972.

Nussbaum, E. S., Djalilian, H. R., Cho, K. H. and Hall, W. A. (1996). Brain metastases: Histology, multiplicity, surgery, and survival. *Cancer* **78**, 1781–1788.

Osborn, L., Hession, C., Tizard, R., Vassallo, C., Luhowskyj, S., Chi-Rosso, G. and Lobb, R. (1989). Direct expression cloning of vascular cell adhesion molecule 1, a cytokine-induced endothelial protein that binds to lymphocytes. *Cell* **59**, 1203–1211.

Peng, H.-H., Hodgson, L., Henderson, A. J. and Dong, C. (2005). Involvement of phospholipase-C signaling in melanoma cell-induced endothelial junction disassembly. *Front. Biosci.* **10**, 1597–1606.

Preusser, M., De Ribaupierre, S., Wöhrer, A., Erridge, S. C., Hegi, M., Weller, M. and Stupp, R. (2011). Current concepts and management of glioblastoma. *Ann. Neurol.* **70**, 9–21.

Proebstl, D., Voisin, M.-B., Woodfin, A., Whiteford, J., D'Acquisto, F., Jones, G. E., Rowe, D. and Nourshargh, S. (2012). Pericytes support neutrophil subendothelial cell crawling

and breaching of venular walls in vivo. *J. Exp. Med.* **209**, 1219–34.

Ricard, I., Payet, M. D. and Dupuis, G. (1997). Clustering the adhesion molecules VLA-4 (CD49d/CD29) in Jurkat T cells or VCAM-1 (CD106) in endothelial (ECV 304) cells activates the phosphoinositide pathway and triggers Ca2+ mobilization. *Eur. J. Immunol.* **27**, 1530–1538.

Shasby, D. M., Shasby, S. S., Sullivan, J. M. and Peach, M. J. (1982). Role of endothelial cell cytoskeleton in control of endothelial permeability. *Circ. Res.* **51**, 657–661.

Siegel, R., Miller, K. and Jemal, A. (2015). Cancer statistics , 2015 . *CA Cancer J Clin* **65**, 29.

Smith, W. B., Gamble, J. R., Clark-Lewis, I. and Vadas, M. a (1991). Interleukin-8 induces neutrophil transendothelial migration. *Immunology* **72**, 65–72.

Sporn, M. B. (1996). The war on cancer. *Lancet (London, England)* **347**, 1377–81.

Staunton, D. E., Marlin, S. D., Stratowa, C., Dustin, M. L. and Springer, T. A. (1988). Primary structure of ICAM-1 demonstrates interaction between members of the immunoglobulin and integrin supergene families. *Cell* **52**, 925–933.

Stupp, R., Mason, W. P., van den Bent, M. J., Weller, M., Fisher, B., Taphoorn, M. J., Belanger, K., Brandes, A. A., Marosi, C., Bogdahn, U., et al. (2005). Radiotherapy plus concomitant and adjuvant temozolomide for glioblastoma. *N Engl J Med* **352**, 987–996.

Vestweber, D. (2008). VE-cadherin: The major endothelial adhesion molecule controlling cellular junctions and blood vessel formation. *Arterioscler. Thromb. Vasc. Biol.* **28**, 223–232.

Weis, W. I. and Nelson, W. J. (2006). Re-solving the cadherin-catenin-actin conundrum. *J. Biol. Chem.* **281**, 35593–35597.

Wyckoff, J. B., Jones, J. G., Condeelis, J. S. and Segall, J. E. (2000). A Critical Step in Metastasis : In Vivo Analysis of Intravasation at the Primary Tumor A Critical Step in Metastasis : In Vivo Analysis of Intravasation at the. 2504–2511.